



- 1 Total organic carbon and contribution from speciated organics in cloud water: Airborne data
2 analysis from the CAMP²Ex field campaign
- 3 Connor Stahl¹, Ewan Crosbie^{2,3}, Paola Angela Bañaga^{4,5}, Grace Betito⁴, Rachel A. Braun¹, Zenn
4 Marie Cainglet^{4,5}, Maria Obiminda Cambaliza^{4,5}, Melliza Templonuevo Cruz^{4,6}, Julie Mae
5 Dado⁷, Miguel Ricardo A. Hilario^{4,8}, Gabrielle Frances Leung^{4,9}, Alexander B. MacDonald¹,
6 Angela Monina Magnaye⁷, Jeffrey Reid¹⁰, Claire Robinson^{2,3}, Michael A. Shook², James
7 Bernard Simpas^{4,5}, Shane Marie Visaga^{5,7}, Edward Winstead^{2,3}, Luke Ziemba², Armin
8 Sorooshian^{1,8}
- 9 ¹Department of Chemical and Environmental Engineering, University of Arizona, Tucson,
10 Arizona, 85721, USA
- 11 ²NASA Langley Research Center, Hampton, Virginia, 23666, USA
- 12 ³Science Systems and Applications, Inc., Hampton, Virginia, 23666, USA
- 13 ⁴Air Quality Dynamics-Instrumentation & Technology Development Laboratory, Manila
14 Observatory, Quezon City, 1108, Philippines
- 15 ⁵Department of Physics, School of Science and Engineering, Ateneo de Manila University,
16 Quezon City, 1108, Philippines
- 17 ⁶Institute of Environmental Science and Meteorology, University of the Philippines, Diliman,
18 Quezon City, 1101, Philippines
- 19 ⁷Regional Climate Systems Laboratory, Manila Observatory, Quezon City, 1108, Philippines
- 20 ⁸Department of Hydrology and Atmospheric Sciences, University of Arizona, Tucson, Arizona,
21 85721, USA
- 22 ⁹Department of Atmospheric Science, Colorado State University, Fort Collins, Colorado 80521,
23 USA
- 24 ¹⁰Marine Meteorology Division, Naval Research Laboratory, Monterey, California 93943, USA
- 25 *Correspondence to: armin@email.arizona.edu*



26 Abstract

27 This work focuses on total organic carbon (TOC) and contributing species in cloud water over
28 Southeast Asia using a rare airborne dataset collected during NASA's Cloud, Aerosol and
29 Monsoon Processes Philippines Experiment (CAMP²Ex), in which a wide variety of maritime
30 clouds were studied, including cumulus congestus, altocumulus, altostratus, and cumulus.
31 Knowledge of TOC levels and their contributing species is needed for improved modeling of
32 cloud processing of organics and to understand how aerosols and gases impact and are impacted
33 by clouds. This work relies on 159 samples collected with an Axial Cyclone Cloud water
34 Collector at altitudes of 0.2 – 6.8 km that had sufficient volume for both TOC and speciated
35 organic composition analysis. Species included monocarboxylic acids (glycolate, acetate,
36 formate, and pyruvate), dicarboxylic acids (glutarate, adipate, succinate, maleate, and oxalate),
37 methanesulfonate (MSA), and dimethylamine (DMA). TOC values range between 0.018 –
38 13.660 ppm C with a mean of 0.902 ppm C. The highest TOC values are observed below 2 km
39 with a general reduction aloft. An exception is samples impacted by biomass burning for which
40 TOC remains enhanced as high as 6.5 km (7.048 ppm C). Estimated total organic matter derived
41 from TOC contributes a mean of 30.7% to total measured mass (inorganics + organics).
42 Speciated organics contribute (on carbon mass basis) an average of 30.0% to TOC in the study
43 region, and account for an average of 10.3% to total measured mass.

44 The order of the average contribution of species to TOC, in decreasing contribution of carbon
45 mass, is as follows: acetate ($14.7 \pm 20.5\%$), formate ($5.4 \pm 9.3\%$), oxalate ($2.8 \pm 4.3\%$), DMA
46 ($1.7 \pm 6.3\%$), succinate ($1.6 \pm 2.4\%$), pyruvate ($1.3 \pm 4.5\%$), glycolate ($1.3 \pm 3.7\%$), adipate (1.0
47 $\pm 3.6\%$), MSA ($0.1 \pm 0.1\%$), glutarate ($0.1 \pm 0.2\%$), maleate ($< 0.1 \pm 0.1\%$). Approximately 70%
48 of TOC remains unaccounted for, thus highlighting the complex nature of organics in the study
49 region; samples collected in biomass burning plumes have up to 95.6% of unaccounted TOC
50 mass based on the species detected. Consistent with other regions, monocarboxylic acids
51 dominate the speciated organic mass (~75%) and are about four times in greater abundance than
52 dicarboxylic acids.

53 Samples are categorized into four cases based on back-trajectory history revealing source-
54 independent similarity between the bulk contributions of monocarboxylic and dicarboxylic acids
55 to TOC (16.03% – 23.66% and 3.70% – 8.75%, respectively). Furthermore, acetate, formate,
56 succinate, glutarate, pyruvate, oxalate, and MSA are especially enhanced during biomass burning
57 periods, attributed to peat emissions transported from Sumatra and Borneo. Lastly, dust (Ca^{2+})
58 and sea salt (Na^+/Cl^-) tracers exhibit strong correlations with speciated organics, thus supporting
59 how coarse aerosol surfaces interact with these water-soluble organics.

60



61 1. Introduction

62 The last two decades witnessed an acceleration of research to unravel the nature of the organic
63 fraction of airborne particles, including speciation (Hallquist et al., 2009; Kanakidou et al.,
64 2005), with implications for how particles impact air quality, public health, and the planet's
65 energy balance. However, there has been much less progress on organic research for cloud
66 droplets, owing largely to the inaccessibility of clouds as compared to particles that can be
67 measured more easily near the surface. Analyzing organic matter in cloud water will lead to
68 better understanding of secondary aerosol formation and the nature of cloud condensation nuclei
69 (CCN) that form droplets. The interaction of aerosol particles and clouds interact constitutes the
70 largest uncertainty in estimating total anthropogenic radiative forcing (IPCC, 2013), which
71 motivates using cloud composition as a tool to learn about these processes (MacDonald et al.,
72 2020). Characterizing cloud water composition is insightful for atmospheric chemical processes
73 such as the removal of gases that would otherwise participate in gas-phase reactions and for
74 aqueous reactions that yield products without an efficient gas-phase source (e.g., dicarboxylic
75 acids) (Ervens et al., 2013). While modeling of sulfate production in clouds is fairly mature
76 (Barth et al., 2000; Faloon, 2009; Kreidenweis et al., 2003; Liu et al., 2021), the formation and
77 evolution of organics in cloud water is much more poorly constrained (Ervens, 2015).

78 Advancing this research requires in situ measurements of cloud water composition. Among the
79 most common methods of characterizing the organic fraction of cloud water samples is total
80 organic carbon (TOC) analysis. Whether it is cloud water or fog water, most studies have shown
81 that (i) TOC is enhanced in air masses with higher anthropogenic influence (Collett Jr. et al.,
82 1998; Deguillaume et al., 2014; Herckes et al., 2013; Raja et al., 2009); (ii) ~40% – 85% of the
83 TOC is attributed to unidentified species (Benedict et al., 2012; Boris et al., 2016; Boris et al.,
84 2018; Herckes et al., 2002; Raja et al., 2008); (iii) organic acids usually account for $\leq 15\%$ of the
85 TOC (Deguillaume et al., 2014; Gioda et al., 2011; Straub et al., 2007); (iv) monocarboxylic
86 acids are more abundant than dicarboxylic acids (Löflund et al., 2002); and (v) acetic and formic
87 acids are the most dominant organic acids contributing to TOC (Collett Jr. et al., 2008; Gioda et
88 al., 2011). Most of the aforementioned studies focused on fog, therefore motivating a closer look
89 at cloud water, as solute concentrations depend on the type of aqueous medium (Fig. 1). More
90 specifically, TOC concentrations are reported to be higher in fog water relative to rain water
91 (Kim et al., 2020), while cloud water solute concentrations exceed those in rain water (Decesari
92 et al., 2005; Gioda et al., 2008).

93 Southeast Asia is an ideal laboratory to investigate the nature of TOC and its constituents as it is
94 impacted by a multitude of emissions sources in an environment with persistent cloud cover from
95 a variety of cloud types (e.g., shallow cumulus and cumulus congestus clouds) (Reid et al.,
96 2013). The complex meteorology of the region makes it very difficult to model (Wang et al.,
97 2013; Xian et al., 2013), but simultaneously provides a remarkable opportunity to learn more
98 about how aerosols impact (and are impacted by) tropical cloud systems. A knowledge gap exists
99 as there have been no studies of cloud composition in this region based on airborne
100 measurements. Analysis of fog water at Baengnyeong Island in the eastern Yellow Sea revealed
101 that organic acids accounted for 36 – 69% of TOC (Boris et al., 2016). The Acid Deposition



102 Monitoring Network in East Asia (<https://www.eanet.asia/>) provides data on wet deposition at
103 surface sites such as at the Manila Observatory (Metro Manila, Philippines) (Ma et al., 2021) and
104 is limited to inorganic ions. Previous studies such as the Seven South East Asian Studies
105 (7SEAS) (Reid et al., 2013) and the Cloud, Aerosol and Monsoon Processes Philippines
106 Experiment (CAMP²Ex) weatHER and CompoSition Monitoring (CHECSM) were carried out in
107 this region; however, these campaigns were ground and ship-based, and focused mainly on
108 aerosol particles and not cloud composition (Hilario et al., 2020b; Reid et al., 2015; Reid et al.,
109 2016).

110 Recent studies in Metro Manila, Philippines provide the following results of relevance to this
111 work: (i) a third to a half of the total aerosol particle mass is often unaccounted for after
112 considering water-soluble species (inorganic and organic acid ions and elements) and black
113 carbon (Cruz et al., 2019; Stahl et al., 2020); (ii) organic acids account for less than 1% of total
114 aerosol mass, with oxalate being the most abundant acid (Stahl et al., 2020); (iii) organic acid
115 levels are more enhanced during biomass burning periods (Hilario et al., 2020a), especially
116 succinate and oxalate (Braun et al., 2020; Stahl et al., 2020); and (iv) wet deposition samples
117 clearly show the influence of biomass burning tracer species on cloud composition (Ma et al.,
118 2021). Based on these points, we test two hypotheses: (i) the relative contribution of organic
119 acids to TOC will exceed what was observed at the surface layer over Metro Manila owing to
120 more aged air masses aloft as compared to the surface layer in Metro Manila exposed to fresher
121 emissions; and (ii) clouds impacted by biomass burning emissions will exhibit chemical profiles
122 shifted to higher TOC levels and with a greater portion of that TOC accounted for by organic
123 acids. To address these hypotheses in addition to characterizing the organic fraction of cloud
124 water, we utilized a rich set of cloud water samples collected around the Philippines during
125 CAMP²Ex between August and October in 2019. The subsequent results and discussion focus on
126 TOC concentrations in addition to the relative contribution and interrelationships between a suite
127 of organic species (organic acids, methanesulfonate, dimethylamine) spatially, and as a function
128 of altitude and air mass source origin. A unique aspect of this dataset is the large sample number
129 with both TOC and speciated organic acid information from an airborne platform.

130

131 **2. Methods**

132 **2.1 Study overview**

133 A total of 159 cloud water samples were collected on the NASA P-3B Orion aircraft across 19
134 research flights (RF; 23 August – 5 October 2019) during CAMP²Ex that were measured for
135 ions, pH, and TOC. Flights were based out of Clark International Airport (15.189°N, 120.547°E)
136 and extended to regions around the island of Luzon (Fig. 2). Cloud water samples were collected
137 over a wide range of altitudes ranging from 0.2 – 6.8 km.

138

139 **2.2 Cloud water collection and handling**



140 Samples were collected using the Axial Cyclone Cloud water Collector (AC3), (Crosbie et al.,
141 2018), which efficiently collects cloud droplets with effective diameters $> 20 \mu\text{m}$. The AC3 has a
142 shutter attached to a servo motor allowing the collector to be closed when not in a cloud to
143 prevent contamination. Samples were collected between 10 seconds and 10 minutes depending
144 on cloud availability and liquid water content (i.e., shorter times possible with higher liquid
145 water content). Cloud water was collected in prewashed 15-mL plastic conical vials. Due to
146 thorough prewashing of the plastic conical vials, leaching of organics into samples was
147 negligible. Before each flight, the collector was flushed with $\sim 1 \text{ L}$ of ultra-purified Milli-Q
148 water ($18.2 \text{ M}\Omega\text{-cm}$) prior to obtaining two blank samples. Blanks were also collected post-flight
149 that were similarly flushed prior to being collected. During flight, samples were collected and
150 stored in a cooler with sufficient ice packs to reduce possible decomposition. After flights,
151 samples were immediately taken to an onsite laboratory where sample volumes were recorded
152 and analyzed for ionic composition, TOC, and pH. A background was subtracted from the
153 samples based on the 10th percentile of all samples and blanks collected during the campaign.
154 Excess samples were stored in a refrigerator for future analyses that are outside the scope of this
155 study.

156

157 **2.3 Cloud water analysis**

158 **2.3.1 Ion chromatography**

159 Cloud water was speciated using ion chromatography (IC; Dionex ICS-2100) immediately after
160 each flight to reduce the possibility of degradation of the samples. Measured anionic species of
161 interest were glycolate, acetate, formate, methanesulfonate, pyruvate, glutarate, adipate,
162 succinate, maleate, oxalate, Cl^- , NO_2^- , Br^- , NO_3^- , and SO_4^{2-} . Measured cations were Na^+ , NH_4^+ ,
163 K^+ , dimethylamine (DMA), Mg^{2+} , and Ca^{2+} . A 23-minute instrument method was used for both
164 anion and cation columns with a 2-minute equilibration period, yielding a 25-minute sampling
165 period per sample. The instrument flow rate was 0.4 mL min^{-1} . The anions were measured using
166 a Dionex IonPac AS11-HC $2 \times 250 \text{ mm}$ column, a Dionex AERS 500e suppressor, and with
167 potassium hydroxide as the eluent. The cations were measured using a Dionex IonPac CS12A
168 $2 \times 250 \text{ mm}$ column, a Dionex CERS 500e suppressor, and using methanesulfonic acid (MSA) as
169 the eluent. The instrument methods used for analysis are as follows: (i) for anions the eluent
170 concentration started at 1 mM, ramped up to 4 mM between 0 – 10 minutes, ramped up to 6 mM
171 between 10 – 11 minutes, and finally ramped up to 7 mM between 11 – 23 minutes using a
172 suppressor current of 8 mA; (ii) for cations the eluent concentration started at 5 mM and
173 remained isocratic from 0 – 10 minutes, ramped up to 18 mM between 10 – 12 minutes, and
174 finally remained isocratic at 18 mM from 12 – 23 minutes using a suppressor current of 22 mA.
175 The limits of detection (LOD) for these species can be found in Table 1.

176

177 **2.3.2 Total organic carbon**

178 Total organic carbon (TOC) was measured using a Sievers 800 Turbo TOC analyzer. Sample
179 aliquots were diluted to obtain the minimum volume needed by the instrument. The TOC



180 analyzer was operated in turbo mode and TOC values were averaged over a stable concentration
181 period. Milli-Q water was used as an internal reference and calibrations were performed before
182 and after each batch of samples was analyzed (i.e., one batch every ~3 – 4 flights) using a range
183 of different concentrations from an oxalate standard solution. A volume of approximately 10 mL
184 was used for each measurement and MQ water was used intermittently to flush the instrument
185 between each sample.

186

187 **2.3.3 Units**

188 While many studies report concentrations in terms of air-equivalent concentrations, we instead
189 use the native liquid-phase concentrations. Aqueous concentrations of TOC and individual
190 molecular components are reported in units of ppb (i.e., parts per billion by mass). TOC
191 concentrations are specific to the mass of carbon atoms only, while molecules measured by IC
192 correspond to the specific mass of the species (unless noted otherwise). TOC was converted to
193 total organic matter (TOM) via multiplication by 1.8 (Zhang et al., 2005).

194 The choice to focus on aqueous- rather than air-equivalent concentrations was made for various
195 reasons. First, our analysis focuses heavily on relative amounts of species that were unaffected
196 by multiplying native aqueous units by cloud liquid water content. Second, the definition of
197 liquid water content applied by studies can vary widely based on the lower and upper bound of
198 what is considered a droplet. Third, relationships between solute concentrations in cloud water
199 and liquid water content, anticipated from nucleation scavenging, are ineffective when gases like
200 acetic and formic acids adsorb directly to droplets rather than having been part of the initial CCN
201 activating into droplets (Khare et al., 1999; Marinoni et al., 2004). Lastly, many studies of cloud
202 water composition that our results can be contrasted with also use liquid units. The primary
203 liquid units reported for cloud water concentrations are ppm and ppb.

204

205 **2.4 Aerosol Composition**

206 To complement the cloud water composition results, we use aerosol composition results from the
207 High-Resolution Time-of-Flight Aerosol Mass Spectrometer (AMS; Aerodyne, Inc.), which
208 reports non-refractory composition for the submicrometer range (DeCarlo et al., 2006). As
209 summarized by Hilario et al. (2021), the AMS deployed in CAMP²Ex functioned in 1 Hz Fast-
210 MS mode with data averaged to 30 s time resolution with the lower limit of detection (units of
211 $\mu\text{g m}^{-3}$) as follows for the measured species: organic (0.169), NH_4^+ (0.169), SO_4^{2-} (0.039), NO_3^-
212 (0.035), Cl^- (0.036). Negative mass concentrations were recorded owing to the difference method
213 used with the limits of detection. These negative values were included in the analyses to avoid
214 positive biases but were interpreted as zero concentrations. We also use data specifically for the
215 mass spectral marker representative of acid-like oxygenated organic species (m/z 44= COO^+)
216 (Aiken et al., 2008) and its mass relative to total organic mass (f_{44}). AMS data were omitted from
217 analysis if total mass of all detected species was $< 0.5 \mu\text{g m}^{-3}$. By convention for airborne
218 sampling, AMS data are reported at standard temperature and pressure (STP; 273 K, 1013 hPa).



219 AMS data were reported separately for cloud-free and cloudy conditions owing to the use of a
220 counterflow virtual impactor (CVI) inlet (Brechtel Manufacturing Inc.) (Shingler et al., 2012) in
221 clouds to isolate and dry droplets, leaving the residual particles for sampling by the AMS. Cloud-
222 free data involve sampling with a separate inlet designed by the University of Hawaii
223 (McNaughton et al., 2007). For cloud-free AMS results, data were selected 60 seconds before
224 and after each cloud water sample's start and end time, respectively, when the aircraft was not in
225 cloud. CVI-AMS data were reported for data collected within the period of cloud water
226 collection. It should be noted that cloud-free AMS data are missing for some cloud water
227 samples when the CVI was still in use for the 60 s before and after a sample's start and end time,
228 respectively.

229

230 **2.5 HYSPLIT**

231 Air mass origination was determined using 5-day back trajectories from the National Oceanic
232 and Atmospheric Administration (NOAA) Hybrid Single Particle Lagrangian Integrated
233 Trajectory model (HYSPLIT) (Rolph et al., 2017; Stein et al., 2015). Trajectories were generated
234 at 1-minute temporal resolution with meteorological inputs from the Global Forecast System
235 (GFS) reanalysis with a horizontal resolution of $0.25^\circ \times 0.25^\circ$ using the "model vertical velocity"
236 method.

237

238 **2.6 NAAPS**

239 The Navy Aerosol Analysis and Prediction System (NAAPS) global aerosol model was
240 implemented to assist in identifying biomass burning cases (Lynch et al., 2016)
241 (<https://www.nrlmry.navy.mil/aerosol/>). NAAPS relies on global meteorological fields from the
242 Navy Global Environmental Model (NAVGEM) (Hogan and Brody, 1993; Hogan and Rosmond,
243 1991) that analyzes and forecasts a $1^\circ \times 1^\circ$ grid with 6-hour intervals with 24 vertical levels. In
244 terms of identifying biomass burning cases, surface smoke concentrations were examined.
245

246 **3. Cumulative Results**

247 **3.1 Concentration Statistics**

248 TOC values ranged from 0.018 – 13.660 ppm C, with median and mean levels of 0.546 and
249 0.902 ppm C, respectively (Table 1). Samples in this study exhibited nearly the lowest mean
250 TOC value of all cloud water studies surveyed in Fig. 1, with the other lowest values being in
251 San Diego, California (0.85 ppm C), (Straub et al., 2007) and East Peak, Puerto Rico (0.90 ppm
252 C), (Gioda et al., 2008; Gioda et al., 2011; Reyes-Rodríguez et al., 2009). The CAMP²Ex dataset
253 exhibited the lowest minimum TOC value of all shown studies. For context, the highest mean
254 and maximum TOC levels in cloud water studies were 34.5 and 51.7 ppm C, respectively, at Jeju
255 Island, Korea, while the peak dissolved organic carbon (DOC) level in cloud water was 85.6 ppm
256 C at Mt. Tai, China. For comparisons to published cloud water measurements, DOC and TOC
257 are assumed to be sufficiently similar in nature to directly compare values. Differences in TOC



258 between our study and others can partly be attributed to the different types of clouds studied in
259 the CAMP²Ex region (e.g., cumulus congestus, cumulus, altocumulus, altostratus) and the higher
260 collection altitudes being conducive to enhanced liquid water contents and droplet sizes than
261 stratocumulus clouds in regions like the northeastern (Straub et al., 2007) and southeastern
262 Pacific Ocean (Benedict et al., 2012). Previous studies have primarily sampled stratocumulus or
263 stratus clouds (Fig. 1). Also, some of our samples may have included rain water, which naturally
264 has lower levels of TOC than cloud water due to dilution (Fig. 1). To illustrate the importance of
265 this dilution effect, an average of the mean values from the Fig. 1 studies shows the following
266 (ppm C): Fog = 17.8, cloud = 6.4, rain = 0.6. We further note that direct comparisons of our
267 results to others need to factor that water collectors have different transmission efficiency
268 behavior as a function of droplet size.

269 The order of species is as follows in terms of decreasing average contribution of C mass relative
270 to total TOC: acetate ($14.7 \pm 20.5\%$), formate ($5.4 \pm 9.3\%$), oxalate ($2.8 \pm 4.3\%$), DMA ($1.7 \pm$
271 6.3%), succinate ($1.6 \pm 2.4\%$), pyruvate ($1.3 \pm 4.5\%$), glycolate ($1.3 \pm 3.7\%$), adipate ($1.0 \pm$
272 3.6%), MSA ($0.1 \pm 0.1\%$), glutarate ($0.1 \pm 0.2\%$), and maleate ($< 0.1 \pm 0.1\%$). An average of
273 70.0% of TOC mass went unaccounted for. The predominant sources and production pathways
274 of these species are briefly explained here. Precursor emissions sources for acetate and formate
275 include plants, soil, vehicles, and biomass burning, with key production routes including
276 oxidation of isoprene, ozonolysis of olefins, and peroxy radical reactions (Khare et al., 1999, and
277 references therein). Pyruvate is considered the most abundant aqueous reaction product of
278 methylglyoxal, generated by the oxidation of gas-phase anthropogenic volatile organic
279 compounds (Boris et al., 2014; Carlton et al., 2006; Lim et al., 2013; Stefan et al., 1996; Tan et
280 al., 2010). Glycolate has been linked to aqueous processing of acetate and a precursor for
281 glyoxylate (Boris et al., 2014) and formed via oxidation of glycolaldehyde by hydroxide radicals
282 (Thomas et al., 2016). Oxalate is the most abundant dicarboxylic acid across different
283 environments (Cruz et al., 2019; Stahl et al., 2020; Yang et al., 2014; Ziemba et al., 2011) and
284 can be emitted directly by biogenic sources (Boone et al., 2015; Kawamura and Kaplan, 1987),
285 combustion exhaust (Kawamura and Kaplan, 1987; Kawamura and Yasui, 2005), and biomass
286 burning (Narukawa et al., 1999; Yang et al., 2014); however, it is also formed through the
287 oxidation and degradation of longer chain organic acids and acts as a notable tracer for cloud
288 processing (Ervens et al., 2004; Sorooshian et al., 2006). Saturated organics like glutarate,
289 adipate, and succinate are linked to fresh emissions and mainly from ozonolysis of cyclic alkenes
290 (such as from vehicular emissions) in the study region (Hatakeyama et al., 1985; Stahl et al.,
291 2020). Maleate can be secondarily formed from the photooxidation of benzene (Rogge et al.,
292 1993) or from the primary emissions of combustion engines (Kawamura and Kaplan, 1987).
293 Alkyl amines (i.e., DMA) have numerous sources such as biomass burning, vehicular emissions,
294 industrial activity, animal husbandry, waste treatment, and the ocean (Youn et al., 2015). Finally,
295 MSA is formed via photooxidation reactions involving dimethylsulfide (DMS) from oceanic
296 emissions (Berresheim, 1987; Saltzman et al., 1983) or dimethyl sulfoxide (DMSO) from
297 anthropogenic emissions (Yuan et al., 2004), in addition to being linked to agricultural emissions
298 and biomass burning (Sorooshian et al., 2015).



299 Measured organic species were further grouped into categories: monocarboxylic acids (MCA;
300 glycolate, acetate, formate, pyruvate), dicarboxylic acids (DCA; glutarate, adipate, succinate,
301 maleate, oxalate), and measured organics (MO = sum of MCA, DCA, MSA, DMA). Total MCA
302 concentrations accounted on average for ~75% of MO and were approximately four times larger
303 than those of DCAs. MO values ranged from 29.5 – 10815.3 ppb, accounting for an average of
304 30.0% (median 23.8%) of TOC when masses were converted to just the C masses of the
305 measured species (Table 1). Examples of other undetected organics include tricarboxylic acids,
306 aromatics, alcohols, sugars, carbohydrates, and aldehydes. Previous studies reported undetected
307 species accounting for ~45% (Boris et al., 2016) and 82.9% (Boris et al., 2018) of organics.
308 Interestingly, the ionic charge balance for the 159 samples shows a slight cation deficit (Fig. S1),
309 with a slope of 1.04 (i.e., anion charge on y-axis). This fairly good charge balance suggests that
310 detected organic species were balanced by cations detected via IC analysis. Species contributing
311 to the slight cation deficit likely include metal cations and H⁺.

312 TOC was converted to total organic matter (TOM) by multiplying it by 1.8 (Zhang et al., 2005),
313 as in other cloud water studies (Boris et al., 2016; Boris et al., 2018), in order to compare it to
314 total measured mass (i.e., sum of TOM, Na, NH₄⁺, K⁺, Mg²⁺, Ca²⁺, Cl⁻, NO₂⁻, Br⁻, NO₃⁻, SO₄²⁻).
315 We caution that using a fixed 1.8 conversion value yields uncertainty as samples were collected
316 in a range of air masses, but 1.8 is a value fairly intermediate to those reported in the literature:
317 1.6 ± 0.2 for urban aerosols (Turpin and Lim, 2001), 2.07 ± 0.05 in nonurban areas (Yao et al.,
318 2016), and values for biomass burning organic aerosols ranging from 1.56 – 2.0 (Aiken et al.,
319 2008; Turpin and Lim, 2001) based on fuel type and combustion condition (Aiken et al., 2008).
320 Higher values are expected for more oxidized organics. Estimated TOM accounted for a median
321 and mean of 23.2% and 30.7%, respectively, of total measured mass, with the maximum for a
322 single sample being 95.1%. The median and mean ratios of MO to TOM were 38.1% and 46.4%,
323 respectively. Furthermore, the median and mean ratios of MO to total measured mass were 7.2%
324 and 10.3%, respectively, with a maximum of 57.6%. On average, chloride, sulfate, and nitrate
325 were the most abundant species (≥ 12.6%), with the median and mean ratio of total inorganic
326 mass to TOM being 3.3 and 5.8, respectively.

327 Our calculated percentages of MO relative to total measured mass are in contrast to results from
328 a surface site in Metro Manila (Stahl et al., 2020), where most of the same organic species
329 (adipate, succinate, maleate, oxalate, MSA) accounted for < 1% of total aerosol mass. Therefore,
330 the first hypothesis of this study holds true that the contributions of measured organic species
331 account for a greater portion of total measured mass in cloud water as compared to surface
332 particulate matter.

333 Gravimetry was used to measure total mass in the surface measurements whereas in cloud water,
334 total measured mass was more restrictive in terms of being based on measurable species, thus
335 qualifying our percentages as an upper bound. However, the measured ions in cloud water should
336 contribute relatively more to total measured mass in cloud water owing to their hygroscopic
337 nature and greater ease to become associated with cloud water as compared to more hydrophobic
338 species like black carbon that contribute significantly to total aerosol mass in the boundary layer
339 of Metro Manila. For example, black carbon accounted for 78.1% and 51.8% of the total mass



340 between 0.10 – 0.18 μm and 0.18 – 0.32 μm in Metro Manila surface aerosol particles (Cruz et
341 al., 2019), respectively, size ranges of which are highly relevant to droplet activation. Air masses
342 aloft in the CAMP²Ex region, and especially those processed by clouds, are likely more aged and
343 oxidized compared to fresh organic emissions (e.g., automobiles, industry, burning) in the
344 surface layer over Metro Manila, which is the most populated urban area within the CAMP²Ex
345 flight domain. Recent work has shown that cloud processing of isoprene oxidation products (a
346 key fraction of organic precursor vapors involved with organic aerosol generation) is the main
347 source of secondary organic aerosol (SOA) in the mid-troposphere (4 – 6 km) (Lamkaddam et
348 al., 2021). This motivates examining vertical TOC and organic species characteristics in more
349 detail, which is discussed next.

350

351 **3.2 Vertical Profiles**

352 The vertical profile of TOC levels was of interest as it relates to general vertical distribution of
353 organic matter in the troposphere. Measurements off the coast of Japan approximately two
354 decades ago during the ACE-Asia campaign revealed unexpectedly high organic aerosol levels in
355 the free troposphere due to presumed SOA formation (Heald et al., 2005). During that campaign,
356 organic aerosol concentrations in the boundary layer and free troposphere, and their relative
357 contribution to total non-refractory aerosol mass (organic, SO_4^{2-} , NO_3^- , NH_4^+), were amongst the
358 highest of various global regions examined (Heald et al., 2011). Therefore, it is of interest to
359 examine such types of vertical profiles farther south in the CAMP²Ex region where data are
360 more scarce, with the unique aspect of this work being the focus on cloud water composition.

361 The highest TOC levels were observed in the bottom two kilometers, with a general reduction
362 above that altitude (Fig. 3). The decrease of TOC concentration with respect to altitude could be
363 attributed to more dilution in larger droplet sizes; results of cloud microphysical data will be the
364 focus of forthcoming work. Four data points influenced by biomass burning were singled out in
365 red markers (Fig. 3a) owing to having systematically higher TOC levels than other points. Those
366 points will be discussed in more detail in Sect. 4, and it is noteworthy that clouds were impacted
367 by biomass burning across a wide range of altitudes up to almost 7 km.

368 Focusing on the non-biomass burning (non-BB) data, there was considerable variation in the
369 bottom 2 km in TOC, with levels as low as 0.144 ppm C and as high as 3.362 ppm C.
370 Interestingly, cloud water collected above 5 km tended to still show enhanced TOC levels,
371 reaching up to 1.530 ppm C (6.1 km) among the non-BB points. The composition contributing to
372 TOC was similar with altitude in non-BB and biomass burning (BB) conditions, with ~75% of
373 TOC mass unaccounted for by the measured species, and MCAs dominating the measured
374 organic mass (Fig. 3b). The exception to that was the high-altitude BB point where 95.6% of
375 TOC was unassigned. Fig. 3c-d show that there was some qualitative agreement in the vertical
376 profile of AMS organic and m/z 44 for data collected immediately adjacent to the cloud water
377 samples in cloud-free air; more specifically, the highest levels of AMS organic, m/z 44, and TOC
378 were in the bottom 2 km. However, some interesting differences exist as they related to specific
379 air mass types as will be discussed in Sect. 4. Some differences could be rooted in how AMS



380 data represent submicrometer particles whereas cloud water data encompass a wider range of
381 particle sizes that activated into cloud droplets (including supermicrometer dust and sea salt
382 particles) and also gases partitioning to cloud water.

383 Vertical profiles of ratios representative of the relative amount of oxidized organics are shown in
384 Fig. 4. The MO:TOC ratio was quite variable with altitude ranging from 0.16 to 0.32 based on
385 the locally averaged curve shown; individual sample values ranged from 0.01 to 0.92. Vertically-
386 resolved ratio values for f_{44} in cloud-free air and in cloud (downstream CVI) ranged on average
387 between 0 to 0.35 and 0.13 to 0.35, respectively. While mass concentrations decreased with
388 altitude (Fig. 3), ratios relevant to the degree of organic aerosol oxidation and make-up of the
389 organic component of cloud water did not exhibit a clear change with altitude.

390

391 **4. Case Studies**

392 Four subsets of samples are examined here to probe how the organic nature of cloud water varies
393 for distinct air masses. Sources of the air masses are visually shown in Fig. 5 based on 5-day
394 HYSPLIT back-trajectories: (i) “North” (RF11, $n = 20$) collected off the northern coast of Luzon
395 with influence from East Asia, the Korean Peninsula, and Japan; (ii) “East” (RF13, $n = 11$)
396 collected off the eastern coast of Luzon with back-trajectories traced to southern China with
397 subsequent passage across Luzon before arriving to the area of sample collection; (iii) “Biomass
398 Burning” (RF09, $n = 4$) collected to the southwest of Luzon above the Sulu Sea with influence
399 from biomass burning plumes from Borneo and Sumatra primarily consisting of peat as the fuel
400 type (Field and Shen, 2008; Levine, 1999; Page et al., 2002; Stockwell et al., 2016; Xian et al.,
401 2013); and (iv) “Clark” (RF04, RF06, RF07, RF09, RF10, and RF11, $n = 25$) collected around
402 the operational area over Luzon, approximately ~90 km northwest of Metro Manila, with back-
403 trajectories extending to the west and southwest of Luzon.

404 Biomass burning samples were identified based on the following criteria: flight scientist notes,
405 elevated surface smoke concentrations and aerosol optical depth (AOD) from the NAAPS model,
406 and the remarkable enhancement in chemical concentrations in cloud water. TOC, K^+ , SO_4^{2-} , and
407 NH_4^+ in particular were enhanced in these samples with levels exceeding 4 ppm C, 0.13 ppm, 2.3
408 ppm, and 2.5 ppm, respectively.

409 Vertical profile results shown previously (Figs. 3-4) show markers corresponding to these four
410 case studies. With the exception of one BB sample collected at 6.5 km, samples in the four cases
411 were obtained below 3.3 km.

412 **4.1 North**

413 This category of samples was unique in that the mean MO (527.48 ± 301.59 ppb) and TOC (636
414 ± 230 ppb C) concentrations were the lowest of all four cases (Table 2). The largest three organic
415 contributors to TOC were acetate (177.82 ± 72.96 ppb C; $11.5 \pm 4.0\%$), oxalate (148.67 ± 81.47
416 ppb C; $6.0 \pm 1.3\%$), and formate (83.16 ± 79.65 ppb C; $3.0 \pm 2.2\%$). Maleate and DMA were not
417 detected for this case and 73.3% of the TOC went unaccounted for. Samples in this category



418 were collected between 1.2 and 2.9 km, without any pronounced organic chemical trends with
419 altitude (Figs. 3-4).

420 This case exhibited a few distinct features worth noting. First, it had the highest sea salt presence
421 based on the highest case-wide levels of Na^+ (3238 ± 2861 ppb), Cl^- (5277 ± 4333 ppb), Mg^{2+}
422 (347 ± 328 ppb), and Br^- (16 ± 8 ppb), the latter of which is a trace component of sea salt
423 (Seinfeld and Pandis, 2016). MSA originates partly from marine emissions of DMS, but its
424 concentration was among the lowest of all species for all four cases with a mass contribution to
425 total TOC (based on C mass) of only $0.17 \pm 0.05\%$ in the North category (Table 3). In their
426 analysis of aerosol data in the surface layer of Metro Manila, Stahl et al. (2020) showed lower
427 overall organic acid aerosol concentrations in the northeast monsoon season where northeasterly
428 air masses originated predominantly from East Asia; Stahl et al. (2020) also showed those air
429 masses were characterized by an enhancement in organic acid levels in the supermicrometer size
430 range owing to adsorption to coarse particle types such as sea salt and dust, but with a preference
431 for dust (Mochida et al., 2003; Rinaldi et al., 2011; Sullivan and Prather, 2007; Turekian et al.,
432 2003). As there was no direct evidence of dust in this case as the $\text{Ca}^{2+}:\text{Na}^+$ ratio was on average
433 (0.04) nearly the same as sea salt (0.038) (Seinfeld and Pandis, 2016), organic acids could have
434 interacted with sea salt. There were strong correlations between sea salt constituents, TOC, and
435 almost all detected organics (Table S1).

436 The second notable feature of this case was limited air mass aging characteristics based on
437 speciated ratios. The acetate:formate ratio is often used to indicate the relative influence of fresh
438 emissions (higher ratios) as compared to secondary production (lower ratios) (Talbot et al., 1988;
439 Wang et al., 2007). In at least one study, fresh emissions were linked to cloud water ratios above
440 1.5 and aged samples having values below 1 (Coggon et al., 2014). The mean acetate:formate
441 ratio for this air mass category was 4.21 ± 3.26 , which was the highest of all four categories in
442 Table 2, suggestive of fresh emissions and low aging. This was consistent with the $\text{Cl}^-:\text{Na}^+$ ratio
443 (1.70 ± 0.13) being the close to sea water (1.81); our use of this ratio in the study assumes these
444 species originate primarily from sea salt. Lower $\text{Cl}^-:\text{Na}^+$ values in the study region coincide with
445 sea salt reactions with acids such as sulfuric, nitric, and organic acids (AzadiAghdam et al.,
446 2019). This was one of the two cases that had adipate present, with this category exhibiting the
447 highest mean concentration (5.15 ± 6.27 ppb). This suggests there was influence from cyclic
448 organics possibly originating from combustion sources, among others, during the transport to the
449 sample region. Adipate exhibited negative correlations with almost all other organic species in
450 this case (r : -0.48 – -0.72), suggestive of limited aging to form shorter chain carboxylic acids via
451 photochemical reactions (Table S1). With the exception of adipate, interrelationships between
452 the other organics detected in this case exhibited positive and significant correlations with one
453 another suggestive of common precursors and/or production mechanisms. Therefore, the results
454 of the North case point to influences from marine emissions and limited aging signatures based
455 on speciated ratios.

456

457 **4.2 East**



458 The dominant organic contributors to TOC (1051 ± 331 ppb C) in the East case were the same as
459 the North case with the difference being the order after acetate: acetate (359.04 ± 40.71 ppb; 14.9
460 $\pm 3.1\%$), formate (258.18 ± 122.19 ppb; $7.2 \pm 3.8\%$), and oxalate (153.63 ± 81.06 ppb; $3.8 \pm$
461 1.2%). The percentage of TOC unaccounted for by the speciated measurements (69.4%) was the
462 lowest out of all of the cases. This case resembled the North one in that there was marine
463 influence, but with differences being more pronounced dust influence and greater evidence of
464 aging based on chemical ratios. Marine signatures come from the second highest levels of Na^+ ,
465 Cl^- , and Mg^{2+} after North, with high correlations between these species (Table S2).

466 Unlike the previous case, the $\text{Ca}^{2+}:\text{Na}^+$ ratio (0.10) was elevated from that of typical sea salt
467 (0.038). Wang et al. (2018) showed that East Asian dust can get lofted up during dust storms,
468 which could contribute to the transport to the Philippines. Previous studies have shown that
469 organic acids adsorb more readily to dust as compared to sea salt due to dust's more alkaline
470 nature (Stahl et al., 2020; Sullivan and Prather, 2007). While Ca^{2+} was correlated to six of the 11
471 organic species for this case ($r: 0.70 - 0.96$; Table S2), the magnitude of the correlations was
472 very similar to those between either Na^+ or Cl^- and the speciated organics. TOC also exhibited
473 similar correlations with Na^+ , Cl^- , and Ca^{2+} ($r: 0.83 - 0.87$). Therefore, it is too difficult with the
474 given data to assert whether (if at all) the organic acids had a preference towards either salt or
475 dust aerosol particles; of note though is that oxalate exhibited the strongest correlation with
476 either Na^+ , Cl^- , and Ca^{2+} ($r: 0.96 - 0.99$) among all species and also TOC. Additionally, Park et
477 al. (2004) showed enhanced Ca^{2+} and NO_3^- in the coarse mode owing to continental Asian dust.
478 In the East case, speciated organics were fairly well correlated to NO_3^- ($r: 0.68 - 0.99$), which
479 has been associated with adsorption onto coarse aerosol types like dust and sea salt (e.g.,
480 Maudlin et al., 2015; Stahl et al., 2020). Nitrate was especially well correlated with Na^+ , Cl^- , and
481 Ca^{2+} ($r: 0.98 - 1.00$), which exceeded correlations of other common inorganic ions such as SO_4^{2-}
482 and NH_4^+ .

483 The vertical profiles show clearly the systematically higher TOC levels relative to the North case
484 across roughly the same altitude range (1.3 – 3.3 km), but in contrast the AMS organic and m/z
485 44 values (although sparse) were more comparable, which again can simply be due to the
486 differences in what is being measured with AMS not accounting for the supermicrometer
487 particles types (i.e., dust and sea salt) that likely were more influential in the cloud water in the
488 East case.

489 Evidence of greater aging as compared to the North case comes from a few ratios of interest. The
490 $\text{Cl}^-:\text{Na}^+$ ratio for this case (1.40 ± 0.06) was lower than the North case, suggestive of more sea
491 salt reactivity aided by presumed aging. Furthermore, the acetate:formate ratio (1.93 ± 1.51) was
492 less than half the value from the North case. More broadly, the overall contribution of MCAs and
493 DCAs to TOC were very similar between the North and East cases and also the next two cases:
494 $\text{MCA}:\text{TOC} = 16.03\% - 23.66\%$, and $\text{DCA}:\text{TOC} = 3.70\% - 8.75\%$ (Table 3). In contrast to the
495 North case, this category of samples had weaker interrelationships between organic species
496 presumed to be due to the mixture of sources impacting this case including dust, marine
497 particles, and likely other anthropogenic and biogenic sources over land.

498



499 4.3 Biomass Burning

500 The BB category samples exhibited the highest levels of TOC (8342 ± 3730 ppb C) and almost
501 every organic with the dominant contributors to TOC being formate (2177.50 ± 1588.91 ppb; 7.0
502 $\pm 4.5\%$), acetate (1845.21 ± 1667.91 ppb; $8.4 \pm 5.6\%$), and succinate (557.00 ± 575.65 ppb; $2.4 \pm$
503 1.7%). As acetate and formate were so abundant, the relative enhancement of MCA mass was
504 much larger than DCA mass as compared to the three other cases examined (Table 2). While the
505 correlation matrix for this case was quite sparse in terms of significant values owing partly to
506 such few points ($n = 4$), TOC and K^+ were highly correlated ($r: 0.99$), which demonstrates the
507 strong linkage between TOC and biomass burning emissions (Table S3) as also shown by others
508 (Cook et al., 2017). For context, Desyaterik et al. (2013) reported cloud water TOC levels of
509 100.6 ppm C in a biomass burning air mass at Mt. Tai in eastern China that was eight times
510 higher than typical values in the absence of agricultural burning. Cook et al. (2017) observed
511 significant higher cloud water TOC levels during wildfire periods at Whiteface Mountain, New
512 York (16.6 ppm C) than biogenic (2.16 ppm C) or urban (2.11 ppm C) periods.

513 In our BB samples, mean values of succinate (557.00 ± 575.65 ppb), glutarate (150.39 ± 82.20
514 ppb), and pyruvate (125.93 ± 126.12 ppb) were significantly elevated above the other cases.
515 Stahl et al. (2020) recently showed that succinate, oxalate, and MSA were especially enhanced in
516 aerosol samples collected in the study region during BB periods in the 2018 southwest monsoon
517 season. Study-wide peak levels of succinate (1372.00 ppb), oxalate (1135.00 ppb), and MSA
518 (24.79 ppb) were found in this case reinforcing those findings (Stahl et al., 2020). Unlike the
519 previous two cases, maleate was detected in BB samples (5.58 ± 6.46 ppb). Although maleate is
520 associated with combustion sources (Kawamura and Kaplan, 1987; Rogge et al., 1993), such as
521 from extensive ship traffic around the sampling area, other studies have shown enhancements of
522 maleate in BB air masses (i.e., Mardi et al., 2019; Tsai et al., 2013). The percentage of mass
523 contributing to TOC that was unaccounted for was 78.7% , with the highest sample at 6.5 km
524 having 95.6% undetected, which was surprisingly large based on the prevalence of organic acids
525 in biomass burning emissions (Reid et al., 1998). Therefore, the second hypothesis posed in this
526 study is partly true in that the BB case exhibited much higher TOC values; however, these
527 samples did not exhibit a greater contribution by organic acids to TOC since the North and East
528 cases actually had a greater contribution from such species. This motivates more attention to
529 organic chemical speciation in clouds impacted by biomass burning emissions as such a large
530 portion of the TOC mass went unaccounted for in this study.

531 While absolute concentrations of most organics were greatly enhanced, the relative contributions
532 of individual organics within the MCA and DCA subsets of species also varied. Most notably in
533 the MCA category, formate was greatly enhanced with a mass contribution to total MCA mass
534 being 46.40% versus $16.54\% - 29.09\%$ for other cases. In the DCA population of species,
535 glutarate (17.15% versus $0.65\% - 4.02\%$) and succinate (41.95% versus $20.82\% - 38.52\%$)
536 accounted for a higher mass fraction than other cases.

537 The $Cl^-:Na^+$ ratio was 1.30 ± 0.06 and suggestive of Cl^- depletion, which has been observed in
538 other regions with biomass burning and linked to high levels of inorganic and organic acids
539 (Braun et al., 2017, and references therein). This is supported by how the values of MO , SO_4^{2-} ,



540 and NO_3^- were the highest in this case (Table 2). The acetate:formate ratio was 0.69 ± 0.30 , but it
541 is unclear as to how effective this and other ratios are as aging indicators when biomass burning
542 is present and especially as fuel type varies between regions.

543

544 **4.4 Clark**

545 Samples in this category were collected during ascents after takeoff and descents during
546 approaches to the airfield, which allowed for sample collection closer to the surface than the
547 other categories (altitude range: 0.2 – 2.9 km). Clark International Airport is located within the
548 Clark Freeport Zone, which is part of both the Pampanga and Tarlac provinces and consists of
549 five cities and municipalities: Angeles City, Mabalacat City, Porac, Capas, and Bamban. This
550 gives the Clark area a population of approximately 996,000 with a population density of ~ 3100
551 km^{-2} , which is low in comparison to the most populated city in the Philippines, Quezon City in
552 Metro Manila, with 2.94 million people and a population density of $\sim 17000 \text{ km}^{-2}$ (PSA, 2016). In
553 addition to Metro Manila just to the southeast ($\sim 90 \text{ km}$), Clark lies between Mt. Pinatubo to the
554 west and Mt. Arayat to the east, which are active and potentially active volcanoes, respectively.

555 The average TOC for this case ($1181 \pm 920 \text{ ppb C}$) was most similar to the East case and
556 exhibited the most variability relative to the mean TOC value of all four cases, which we
557 attribute to numerous sources impacting these samples including local and regional emissions,
558 time of day variability, local spatial variability, and number of flights. This case exhibited the
559 highest percentage of TOC mass unaccounted for by speciated organics (79.5%) with the three
560 largest measured contributors consisting of acetate ($296.65 \pm 325.80 \text{ ppb}$; $9.6 \pm 9.5\%$), formate
561 ($266.05 \pm 316.80 \text{ ppb}$; $4.8 \pm 3.3\%$), and oxalate ($88.33 \pm 103.88 \text{ ppb}$; $1.7 \pm 1.0\%$). A few notable
562 features are mentioned specific to this case. This was the only case that had DMA present (6.45
563 $\pm 15.89 \text{ ppb}$) albeit with a low mass contribution to total TOC ($0.43 \pm 1.17\%$). This case
564 exhibited the highest mass fractions of maleate ($3.20 \pm 5.93\%$) and adipate ($16.05 \pm 21.48\%$)
565 relative to DCA mass, suggestive of greater anthropogenic emission influence and processed
566 aromatic compounds. DMA was only correlated with maleate ($r: 0.67$) among the organic
567 species suggestive of a similar source (Table S4). Stahl et al. (2020) showed increased aerosol
568 concentrations of freshly emitted organics (i.e., phthalate, maleate) owing to the vast sources of
569 combustion engines to the southeast of the Clark area. Clark is situated near a major highway
570 that could also contribute to the high combustion sources, though commercial aircraft emissions
571 could also have a significant role.

572 Because succinate peaked in concentration for this case (498.50 ppb) and back-trajectories
573 originated from Borneo and Sumatra, there may have been some influence from biomass burning
574 (Fig. 5). The $\text{K}^+:\text{Na}^+$ ratio was elevated (0.25) above that of sea salt (0.036) (Seinfeld and Pandis,
575 2016), and even higher than the Biomass Burning case (0.15), suggestive of local and/or regional
576 biomass burning influence. This case exhibited the highest mean $\text{Ca}^{2+}:\text{Na}^+$ ratio (0.99) that was
577 well above the sea salt value (0.038), which we presume could be linked largely to resuspended
578 and/or transported dust. Cruz et al. (2019) showed for Metro Manila that resuspended dust,
579 especially linked to vehicular traffic, is an important source of dust in the study region. Stahl et



580 al. (2020) showed that adipate is most influenced by crustal sources in the study region and was
581 unique among the studied organics in this work in that it exhibited a prominent peak in the
582 supermicrometer range based on surface aerosol measurements in Metro Manila. Consistent with
583 that work, Ca^{2+} was only correlated with adipate in the Clark samples (r : 0.71) among the studied
584 organics (Table S4), adding support for how organic acids like adipate can partition to dust with
585 the novelty here being that the signature was observed in cloud water.

586

587 5. Conclusion

588 This work analyzed 159 cloud water samples collected over a 2-month period as part of the
589 CAMP²Ex airborne campaign around the Philippines. TOC and a total of eleven organic
590 compounds comprised of four MCAs (glycolate, acetate, formate, and pyruvate), five DCAs
591 (glutarate, adipate, succinate, maleate, and oxalate), MSA, and DMA were measured. The
592 measured organics were then compared to TOC to determine the percentage of organic species
593 measured compared to the total organic composition. Notable results are summarized below
594 including responses to the two hypotheses proposed at the end of Sect. 1.

- 595
- 596 • TOC levels ranged widely between 0.018 – 13.660 ppm C between 0.2 – 6.8 km, with a
597 mean value of 0.902 ppm C. The contribution (in C mass) of the 11 measured species to
598 total TOC was on average 30%. Using a conversion factor of 1.8 for organic matter
599 relative to organic carbon, the mean amount of total organic matter (TOM) accounted for
600 by our measured 11 species was 46.4%. Furthermore, the mean contribution of TOM and
601 speciated organics to total mass (inorganics + organics) was 30.7% (maximum = 95.1%)
602 and 10.3% (maximum = 57.6%), respectively. The mean ratio of inorganic to TOM was
603 5.8. The study's first hypothesis holds true that the measured organic species account for
604 a higher mass fraction relative to total mass as compared to surface layer aerosol
605 measurements over Luzon (< 1%), (Stahl et al., 2020). This is likely owing to more
606 processed air masses aloft and the reduced influence of black carbon that is so abundant
607 in areas like Metro Manila (Cruz et al., 2019; Hilario et al., 2020a).
 - 608 • In terms of the chemical profile of the speciated organics, the order in decreasing
609 contribution of C mass relative to TOC was as follows: acetate ($14.7 \pm 20.5\%$), formate
610 ($5.4 \pm 9.3\%$), oxalate ($2.8 \pm 4.3\%$), DMA ($1.7 \pm 6.3\%$), succinate ($1.6 \pm 2.4\%$), pyruvate
611 ($1.3 \pm 4.5\%$), glycolate ($1.3 \pm 3.7\%$), adipate ($1.0 \pm 3.6\%$), MSA ($0.1 \pm 0.1\%$), glutarate
612 ($0.1 \pm 0.2\%$), maleate ($< 0.1 \pm 0.1\%$). Approximately 70.0% of TOC went unaccounted
613 for pointing to the complexity and difficulty of organic speciation in the study region,
614 with this value fairly similar to other regions too (Benedict et al., 2012; Boris et al., 2016;
615 Boris et al., 2018; Herckes et al., 2002; Raja et al., 2008). Monocarboxylic acids
616 dominated the speciated organic mass (~75%) and were about four times more abundant
617 than dicarboxylic acids, suggestive of higher abundance of gaseous species and
618 precursors.
 - 619 • Vertical profiles of TOC revealed higher levels in the bottom 2 km with a reduction
620 above that. Samples impacted by biomass burning emissions were significantly enhanced
in TOC and most speciated organic levels, ranging in altitude from as low as 1.3 km to as



621 high as 6.5 km. While vertical profiles of AMS organic and m/z 44 qualitatively
622 resembled that of TOC with reductions above 2 km, the vertical behavior of chemical
623 ratios relevant to the composition of the cloud (ratio of C mass from measured organics
624 to TOC) and aerosol organics (f_{44}) did not reveal any clear trend. For both non-BB and
625 BB samples, monocarboxylic acids uniformly dominated C mass with ~75% of TOC
626 mass unaccounted for across the range of altitudes studied.

- 627 • The second hypothesis in this study proved to be partly true as clouds impacted by
628 biomass burning exhibited markedly higher values of TOC (4.974 – 13.660 ppm C) and
629 masses of most all other species detected as compared to the other three categories of
630 samples in Sect. 4 (North, East, Clark). However, the part of the hypothesis about
631 speciated organic acids contributing more to BB samples did not hold true as total
632 measured organics accounted on average for 21.25% of the TOC, which was lower than
633 two of the other categories of samples (North [26.72%] and East [30.61%]). Interestingly,
634 the highest BB sample (6.5 km) had 95.6% of the C mass unaccounted for by speciated
635 organics. This motivates increased attention to organic speciation in clouds impacted by
636 biomass burning.
- 637 • Four categories of samples with different air mass history characteristics were compared
638 revealing a few notable features: (i) while speciated concentrations and TOC levels
639 varied considerably between the four cases, the contributions of MCAs and DCAs (based
640 on C mass) to TOC were remarkably similar with little variation (MCA:TOC = 16.03% –
641 23.66%, DCA:TOC and 3.70% – 8.75%); (ii) dust and sea salt tracer species were
642 strongly correlated to most all speciated organics for the North and East cases suggestive
643 of interactions between such species and coarse aerosol surfaces as supported by past
644 work (Stahl et al., 2020; Sullivan and Prather, 2007); (iii) for samples with limited aging
645 (North case) based on selected chemical ratio values, adipate was more abundant and
646 negatively correlated to smaller carboxylic acids; (iv) BB samples exhibited the highest
647 TOC concentrations (8342 ± 3730 ppb C) as well as significant elevations in individual
648 organics such as acetate, formate, succinate, glutarate, pyruvate, oxalate, and MSA; and
649 (v) the Clark case had a higher variability of TOC (1181 ± 920 ppb C) compared to the
650 North and East cases presumably owing to a greater mix of influential sources such as
651 fresh anthropogenic emissions (e.g., enhanced maleate), but also transport of biomass
652 burning plumes from Borneo and Sumatra (e.g., enhanced succinate), dust, as well as
653 spatial and temporal variances across different flights. Related to dust, Ca^{2+} was only
654 correlated to adipate in the Clark samples, consistent with a recent study in Metro Manila
655 (Stahl et al., 2020) showing that adipate uniquely exhibits a prominent supermicrometer
656 peak among organic acids attributed to interactions with dust.

657

658 **Data availability**

659 All data used can be found on the NASA data repository at
660 DOI:10.5067/Suborbital/CAMP2EX2018/DATA001.

661



662 **Author contributions**

663 EC, RAB, CS, ABM, and AS designed the experiment. All coauthors carried out various aspects
664 of the data collection. EC, CS, and AS conducted analysis and interpretation of the data. CS and
665 AS prepared the manuscript with contributions from the coauthors.

666

667 **Competing interests**

668 The authors declare that they have no conflict of interest.

669

670 **Acknowledgements**

671 The authors acknowledge support from NASA grant 80NSSC18K0148 in support of the NASA
672 CAMP²Ex project. R. A. Braun acknowledges support from the ARCS Foundation. M. Cruz
673 acknowledges support from the Philippine Department of Science and Technology's ASTHRD
674 Program. A. B. MacDonald acknowledges support from the Mexican National Council for
675 Science and Technology (CONACYT).

676

677 **References**

678 Aiken, A. C., Decarlo, P. F., Kroll, J. H., Worsnop, D. R., Huffman, J. A., Docherty, K. S.,
679 Ulbrich, I. M., Mohr, C., Kimmel, J. R., Sueper, D., Sun, Y., Zhang, Q., Trimborn, A.,
680 Northway, M., Ziemann, P. J., Canagratna, M. R., Onasch, T. B., Alfarra, M. R., Prevot, A. S.
681 H., Dommen, J., Duplissy, J., Metzger, A., Baltensperger, U., and Jimenez, J. L.: O/C and
682 OM/OC ratios of primary, secondary, and ambient organic aerosols with high-resolution time-of-
683 flight aerosol mass spectrometry, *Environ. Sci. Technol.*, 42, 4478-4485, 10.1021/es703009q,
684 2008.

685 Anastasio, C., Faust, B. C., and Allen, J. M.: Aqueous phase photochemical formation of
686 hydrogen peroxide in authentic cloud waters, *J. Geophys. Res. Atmos.*, 99, 8231-8248,
687 10.1029/94JD00085, 1994.

688 AzadiAghdam, M., Braun, R. A., Edwards, E.-L., Bañaga, P. A., Cruz, M. T., Betito, G.,
689 Cambaliza, M. O., Dadashazar, H., Lorenzo, G. R., Ma, L., MacDonald, A. B., Nguyen, P.,
690 Simpas, J. B., Stahl, C., and Sorooshian, A.: On the nature of sea salt aerosol at a coastal
691 megacity: Insights from Manila, Philippines in Southeast Asia, *Atmos. Environ.*, 216, 116922,
692 10.1016/j.atmosenv.2019.116922, 2019.

693 Barth, M., Rasch, P., Kiehl, J., Benkovitz, C., and Schwartz, S.: Sulfur chemistry in the National
694 Center for Atmospheric Research Community Climate Model: Description, evaluation, features,
695 and sensitivity to aqueous chemistry, *J. Geophys. Res. Atmos.*, 105, 1387-1415,
696 10.1029/1999JD900773, 2000.



- 697 Benedict, K. B., Lee, T., and Collett Jr, J. L.: Cloud water composition over the southeastern
698 Pacific Ocean during the VOCALS regional experiment, *Atmos. Environ.*, 46, 104-114,
699 10.1016/j.atmosenv.2011.10.029, 2012.
- 700 Berresheim, H.: Biogenic sulfur emissions from the Subantarctic and Antarctic Oceans, *J.*
701 *Geophys. Res. Atmos.*, 92, 13245-13262, 10.1029/JD092iD11p13245, 1987.
- 702 Boone, E. J., Laskin, A., Laskin, J., Wirth, C., Shepson, P. B., Stirm, B. H., and Pratt, K. A.:
703 Aqueous processing of atmospheric organic particles in cloud water collected via aircraft
704 sampling, *Environ. Sci. Technol.*, 49, 8523-8530, 10.1021/acs.est.5b01639, 2015.
- 705 Boris, A., Lee, T., Park, T., Choi, J., Seo, S., and Collett Jr., J.: Fog composition at Baengnyeong
706 Island in the eastern Yellow Sea: detecting markers of aqueous atmospheric oxidations, *Atmos.*
707 *Chem. Phys.*, 16, 437-453, 10.5194/acp-16-437-2016, 2016.
- 708 Boris, A. J., Desyaterik, Y., and Collett Jr., J. L.: How do components of real cloud water affect
709 aqueous pyruvate oxidation?, *Atmos. Res.*, 143, 95-106, 10.1016/j.atmosres.2014.02.004, 2014.
- 710 Boris, A. J., Napolitano, D. C., Herckes, P., Clements, A. L., and Collett Jr., J. L.: Fogs and air
711 quality on the southern California coast, *Aerosol Air Qual. Res.*, 18, 224-239,
712 10.4209/aaqr.2016.11.0522 2018.
- 713 Braun, R. A., Dadashazar, H., MacDonald, A. B., Aldhaif, A. M., Maudlin, L. C., Crosbie, E.,
714 Aghdam, M. A., Mardi, A. H., and Sorooshian, A.: Impact of wildfire emissions on chloride and
715 bromide depletion in marine aerosol particles, *Environ. Sci. Technol.*, 51, 9013-9021,
716 10.1021/acs.est.7b02039, 2017.
- 717 Braun, R. A., Aghdam, M. A., Bañaga, P. A., Betito, G., Cambaliza, M. O., Cruz, M. T.,
718 Lorenzo, G. R., MacDonald, A. B., Simpas, J. B., Stahl, C., and Sorooshian, A.: Long-range
719 aerosol transport and impacts on size-resolved aerosol composition in Metro Manila, Philippines,
720 *Atmos. Chem. Phys.*, 20, 2387-2405, 10.5194/acp-20-2387-2020, 2020.
- 721 Capel, P. D., Gunde, R., Zuercher, F., and Giger, W.: Carbon speciation and surface tension of
722 fog, *Environ. Sci. Technol.*, 24, 722-727, 10.1021/es00075a017, 1990.
- 723 Carlton, A. G., Turpin, B. J., Lim, H.-J., Altieri, K. E., and Seitzinger, S.: Link between isoprene
724 and secondary organic aerosol (SOA): Pyruvic acid oxidation yields low volatility organic acids
725 in clouds, *Geophys. Res. Lett.*, 33, L06822, 10.1029/2005gl025374, 2006.
- 726 Coggon, M., Sorooshian, A., Wang, Z., Craven, J., Metcalf, A., Lin, J., Nenes, A., Jonsson, H.,
727 Flagan, R., and Seinfeld, J.: Observations of continental biogenic impacts on marine aerosol and
728 clouds off the coast of California, *J. Geophys. Res. Atmos.*, 119, 6724-6748,
729 10.1002/2013JD021228, 2014.
- 730 Collett Jr., J. L., Hoag, K. J., Sherman, D. E., Bator, A., and Richards, L. W.: Spatial and
731 temporal variations in San Joaquin Valley fog chemistry, *Atmos. Environ.*, 33, 129-140,
732 10.1016/S1352-2310(98)00136-8, 1998.



- 733 Collett Jr., J. L., Herckes, P., Youngster, S., and Lee, T.: Processing of atmospheric organic
734 matter by California radiation fogs, *Atmos. Res.*, 87, 232-241, 10.1016/j.atmosres.2007.11.005,
735 2008.
- 736 Cook, R. D., Lin, Y.-H., Peng, Z., Boone, E., Chu, R. K., Dukett, J. E., Gunsch, M. J., Zhang,
737 W., Tolic, N., Laskin, A., and Pratt, K. A.: Biogenic, urban, and wildfire influences on the
738 molecular composition of dissolved organic compounds in cloud water, *Atmos. Chem. Phys.*, 17,
739 10.5194/acp-17-15167-2017, 2017.
- 740 Crosbie, E., Brown, M. D., Shook, M., Ziemba, L., Moore, R. H., Shingler, T., Winstead, E.,
741 Thornhill, K. L., Robinson, C., MacDonald, A. B., Dadashazar, H., Sorooshian, A., Beyersdorf,
742 A., Eugene, A., Collett Jr., J., Straub, D., and Anderson, B.: Development and characterization of
743 a high-efficiency, aircraft-based axial cyclone cloud water collector, *Atmos. Meas. Tech.*, 11,
744 5025-5048, 10.5194/amt-11-5025-2018, 2018.
- 745 Cruz, M. T., Bañaga, P. A., Betito, G., Braun, R. A., Stahl, C., Aghdam, M. A., Cambaliza, M.
746 O., Dadashazar, H., Hilario, M. R., Lorenzo, G. R., Ma, L., MacDonald, A. B., Pabroa, P. C.,
747 Yee, J. R., Simpas, J. B., and Sorooshian, A.: Size-resolved composition and morphology of
748 particulate matter during the southwest monsoon in Metro Manila, Philippines, *Atmos. Chem.*
749 *Phys.*, 19, 10675-10696, 10.5194/acp-19-10675-2019, 2019.
- 750 DeCarlo, P. F., Kimmel, J. R., Trimborn, A., Northway, M. J., Jayne, J. T., Aiken, A. C., Gonin,
751 M., Fuhrer, K., Horvath, T., Docherty, K. S., Worsnop, D. R., and Jimenez, J. L.: Field-
752 deployable, high-resolution, time-of-flight aerosol mass spectrometer, *Anal. Chem.*, 78, 8281-
753 8289, 10.1021/ac061249n, 2006.
- 754 Decesari, S., Facchini, M., Fuzzi, S., McFiggans, G., Coe, H., and Bower, K.: The water-soluble
755 organic component of size-segregated aerosol, cloud water and wet depositions from Jeju Island
756 during ACE-Asia, *Atmos. Environ.*, 39, 211-222, 10.1016/j.atmosenv.2004.09.049, 2005.
- 757 Deguillaume, L., Charbouillot, T., Joly, M., Vaïtilingom, M., Parazols, M., Marinoni, A., Amato,
758 P., Delort, A.-M., Vinatier, V., Flossmann, A., Chaumerliac, N., Pichon, J. M., Houdier, S., Laj,
759 P., Sellegri, K., Colomb, A., Brigante, M., and Mailhot, G.: Classification of clouds sampled at
760 the puy de Dôme (France) based on 10 yr of monitoring of their physicochemical properties,
761 *Atmos. Chem. Phys.*, 14, 1485-1506, 10.5194/acp-14-1485-2014, 2014.
- 762 Desyaterik, Y., Sun, Y., Shen, X., Lee, T., Wang, X., Wang, T., and Collett Jr., J. L.: Speciation
763 of “brown” carbon in cloud water impacted by agricultural biomass burning in eastern China, *J.*
764 *Geophys. Res. Atmos.*, 118, 7389-7399, 10.1002/jgrd.50561, 2013.
- 765 Ehrenhauser, F. S., Khadapkar, K., Wang, Y., Hutchings, J. W., Delhomme, O., Kommalapati,
766 R. R., Herckes, P., Wornat, M. J., and Valsaraj, K. T.: Processing of atmospheric polycyclic
767 aromatic hydrocarbons by fog in an urban environment, *J. Environ. Monitor.*, 14, 2566-2579,
768 10.1039/C2EM30336A, 2012.
- 769 Erel, Y., Pehkonen, S. O., and Hoffmann, M. R.: Redox chemistry of iron in fog and stratus
770 clouds, *J. Geophys. Res. Atmos.*, 98, 18423-18434, 10.1029/93JD01575, 1993.



- 771 Ervens, B., Feingold, G., Clegg, S. L., and Kreidenweis, S. M.: A modeling study of aqueous
772 production of dicarboxylic acids: 2. Implications for cloud microphysics, *J. Geophys. Res.*
773 *Atmos.*, 109, D15206, 10.1029/2004jd004575, 2004.
- 774 Ervens, B., Wang, Y., Eagar, J., Leaitch, W., Macdonald, A., Valsaraj, K., and Herckes, P.:
775 Dissolved organic carbon (DOC) and select aldehydes in cloud and fog water: the role of the
776 aqueous phase in impacting trace gas budgets, *Atmos. Chem. Phys.*, 13, 5117-5135,
777 10.5194/acp-13-5117-2013, 2013.
- 778 Ervens, B.: Modeling the processing of aerosol and trace gases in clouds and fogs, *Chem. Rev.*,
779 115, 4157-4198, 10.1021/cr5005887, 2015.
- 780 Faloon, I.: Sulfur processing in the marine atmospheric boundary layer: A review and critical
781 assessment of modeling uncertainties, *Atmos. Environ.*, 43, 2841-2854,
782 10.1016/j.atmosenv.2009.02.043, 2009.
- 783 Field, R. D., and Shen, S. S.: Predictability of carbon emissions from biomass burning in
784 Indonesia from 1997 to 2006, *J. Geophys. Res. Biogeosci.*, 113, G04024,
785 10.1029/2008JG000694, 2008.
- 786 Gelencser, A., Sallai, M., Krivacsy, Z., Kiss, G., and Meszaros, E.: Voltammetric evidence for
787 the presence of humic-like substances in fog water, *Atmos. Res.*, 54, 157-165, 10.1016/S0169-
788 8095(00)00042-9, 2000.
- 789 Gioda, A., Mayol-Bracero, O. L., Reyes-Rodriguez, G. J., Santos-Figueroa, G., and Collett Jr., J.
790 L.: Water-soluble organic and nitrogen levels in cloud and rainwater in a background marine
791 environment under influence of different air masses, *J. Atmos. Chem.*, 61, 85-99,
792 10.1007/s10874-009-9125-6, 2008.
- 793 Gioda, A., Reyes-Rodríguez, G. J., Santos-Figueroa, G., Collett Jr., J. L., Decesari, S., Ramos,
794 M. d. C. K., Bezerra Netto, H. J., de Aquino Neto, F. R., and Mayol-Bracero, O. L.: Speciation
795 of water-soluble inorganic, organic, and total nitrogen in a background marine environment:
796 Cloud water, rainwater, and aerosol particles, *J. Geophys. Res. Atmos.*, 116, D05203,
797 10.1029/2010JD015010, 2011.
- 798 Hadi, D., Crossley, A., and Cape, J.: Particulate and dissolved organic carbon in cloud water in
799 southern Scotland, *Environ. Pollut.*, 88, 299-306, 10.1016/0269-7491(95)93443-4, 1995.
- 800 Hallquist, M., Wenger, J. C., Baltensperger, U., Rudich, Y., Simpson, D., Claeys, M., Dommen,
801 J., Donahue, N., George, C., Goldstein, A., Hamilton, J. F., Herrmann, H., Hoffmann, T., Iinuma,
802 Y., Jang, M., Jenkin, M. E., Jimenez, J. L., Kiendler-Scharr, A., Maenhaut, W., McFiggans, G.,
803 Mentel, T. F., Monod, A., Prevot, A. S. H., Seinfeld, J. H., Surratt, J. D., Szmigielski, R., and
804 Wildt, J.: The formation, properties and impact of secondary organic aerosol: current and
805 emerging issues, *Atmos. Chem. Phys.*, 9, 5155-5236, 10.5194/acp-9-5155-2009, 2009.
- 806 Hatakeyama, S., Tanonaka, T., Weng, J., Bandow, H., Takagi, H., and Akimoto, H.: Ozone-
807 cyclohexene reaction in air: quantitative analysis of particulate products and the reaction
808 mechanism, *Environ. Sci. Technol.*, 19, 935-942, 10.1021/es00140a008, 1985.



- 809 Heald, C., Coe, H., Jimenez, J., Weber, R., Bahreini, R., Middlebrook, A., Russell, L., Jolleys,
810 M., Fu, T.-M., Allan, J., Bower, K. N., Capes, G., Crosier, J., Morgan, W. T., Robinson, N. H.,
811 Williams, P. I., Cubison, M. J., DeCarlo, P. F., and Dunlea, E. J.: Exploring the vertical profile of
812 atmospheric organic aerosol: comparing 17 aircraft field campaigns with a global model, *Atmos.*
813 *Chem. Phys.*, 11, 12673-12696, 10.5194/acp-11-12673-2011, 2011.
- 814 Heald, C. L., Jacob, D. J., Park, R. J., Russell, L. M., Huebert, B. J., Seinfeld, J. H., Liao, H., and
815 Weber, R. J.: A large organic aerosol source in the free troposphere missing from current
816 models, *Geophys. Res. Lett.*, 32, L18809, 10.1029/2005GL023831, 2005.
- 817 Herckes, P., Hannigan, M. P., Trenary, L., Lee, T., and Collett Jr., J. L.: Organic compounds in
818 radiation fogs in Davis (California), *Atmos. Res.*, 64, 99-108, 10.1016/S0169-8095(02)00083-2,
819 2002.
- 820 Herckes, P., Chang, H., Lee, T., and Collett Jr., J. L.: Air pollution processing by radiation fogs,
821 *Water Air Soil Pollut.*, 181, 65-75, 10.1007/s11270-006-9276-x, 2007.
- 822 Herckes, P., Valsaraj, K. T., and Collett Jr., J. L.: A review of observations of organic matter in
823 fogs and clouds: Origin, processing and fate, *Atmos. Res.*, 132-133, 434-449,
824 10.1016/j.atmosres.2013.06.005, 2013.
- 825 Hilario, M. R. A., Cruz, M. T., Bañaga, P. A., Betito, G., Braun, R. A., Stahl, C., Cambaliza, M.
826 O., Lorenzo, G. R., MacDonald, A. B., AzadiAghdam, M., Pabroa, P. C., Yee, J. R., Simpas, J.
827 B., and Sorooshian, A.: Characterizing weekly cycles of particulate matter in a coastal megacity:
828 The importance of a seasonal, size-resolved, and chemically-speciated analysis, *J. Geophys. Res.*
829 *Atmos.*, 125, e2020JD032614, 10.1029/2020JD032614, 2020a.
- 830 Hilario, M. R. A., Cruz, M. T., Cambaliza, M. O. L., Reid, J. S., Xian, P., Simpas, J. B.,
831 Lagrosas, N. D., Uy, S. N. Y., Cliff, S., and Zhao, Y.: Investigating size-segregated sources of
832 elemental composition of particulate matter in the South China Sea during the 2011 Vasco
833 cruise, *Atmos. Chem. Phys.*, 20, 1255-1276, 10.5194/acp-20-1255-2020, 2020b.
- 834 Hilario, M. R. A., Crosbie, E., Shook, M., Reid, J. S., Cambaliza, M. O. L., Simpas, J. B. B.,
835 Ziemba, L., DiGangi, J. P., Diskin, G. S., Nguyen, P., Turk, F. J., Winstead, E., Robinson, C. E.,
836 Wang, J., Zhang, J., Wang, Y., Yoon, S., Flynn, J., Alvarez, S. L., Behrangi, A., and Sorooshian,
837 A.: Measurement report: Long-range transport patterns into the tropical northwest Pacific during
838 the CAMP2Ex aircraft campaign: chemical composition, size distributions, and the impact of
839 convection, *Atmos. Chem. Phys.*, 21, 3777-3802, 10.5194/acp-21-3777-2021, 2021.
- 840 Hogan, T. F., and Rosmond, T. E.: The description of the Navy Operational Global Atmospheric
841 Prediction System's spectral forecast model, *Mon. Weather Rev.*, 119, 1786-1815, 10.1175/1520-
842 0493(1991)119<1786:TDOTNO>2.0.CO;2, 1991.
- 843 Hogan, T. F., and Brody, L. R.: Sensitivity studies of the Navy's global forecast model
844 parameterizations and evaluation of improvements to NOGAPS, *Mon. Weather Rev.*, 121, 2373-
845 2395, 10.1175/1520-0493(1993)121<2373:SSOTNG>2.0.CO;2, 1993.



- 846 Hutchings, J. W., Robinson, M. S., McIlwraith, H., Kingston, J. T., and Herckes, P.: The
847 chemistry of intercepted clouds in Northern Arizona during the North American monsoon
848 season, *Water Air Soil Pollut.*, 199, 191-202, 10.1007/s11270-008-9871-0, 2008.
- 849 IPCC: *Climate Change 2013: The Physical Science Basis*, Cambridge University Press,
850 10.1017/CBO9781107415324, 2013.
- 851 Kanakidou, M., Seinfeld, J., Pandis, S., Barnes, I., Dentener, F. J., Facchini, M. C., Dingenen, R.
852 V., Ervens, B., Nenes, A., Nielsen, C., Swietlicki, E., Putaud, J. P., Balkanski, Y., Fuzzi, S.,
853 Horth, J., Moortgat, G. K., Winterhalter, R., Myhre, C. E. L., Tsigaridis, K., Vignati, E.,
854 Stephanou, E. G., and Wilson, J.: Organic aerosol and global climate modelling: a review,
855 *Atmos. Chem. Phys.*, 5, 1053-1123, 10.5194/acp-5-1053-2005, 2005.
- 856 Kawamura, K., and Kaplan, I. R.: Motor exhaust emissions as a primary source for dicarboxylic
857 acids in Los Angeles ambient air, *Environ. Sci. Technol.*, 21, 105-110, 10.1021/es00155a014,
858 1987.
- 859 Kawamura, K., and Yasui, O.: Diurnal changes in the distribution of dicarboxylic acids,
860 ketocarboxylic acids and dicarbonyls in the urban Tokyo atmosphere, *Atmos. Environ.*, 39,
861 1945-1960, 10.1016/j.atmosenv.2004.12.014, 2005.
- 862 Khare, P., Kumar, N., Kumari, K., and Srivastava, S.: Atmospheric formic and acetic acids: An
863 overview, *Rev. Geophys.*, 37, 227-248, 10.1029/1998RG900005, 1999.
- 864 Kim, H. J., Lee, T., Park, T., Park, G., Collett Jr., J. L., Park, K., Ahn, J. Y., Ban, J., Kang, S.,
865 Kim, K., Park, S.-M., Jho, E. H., and Choi, Y.: Ship-borne observations of sea fog and rain
866 chemistry over the North and South Pacific Ocean, *J. Atmos. Chem.*, 76, 315-326,
867 10.1007/s10874-020-09403-8, 2020.
- 868 Kreidenweis, S. M., Walcek, C. J., Feingold, G., Gong, W., Jacobson, M. Z., Kim, C. H., Liu, X.,
869 Penner, J. E., Nenes, A., and Seinfeld, J. H.: Modification of aerosol mass and size distribution
870 due to aqueous-phase SO₂ oxidation in clouds: Comparisons of several models, *J. Geophys. Res.*
871 *Atmos.*, 108, 4213, 10.1029/2002JD002697, 2003.
- 872 Lamkaddam, H., Dommen, J., Ranjithkumar, A., Gordon, H., Wehrle, G., Krechmer, J., Majluf,
873 F., Salionov, D., Schmale, J., Bjelić, S., Carslaw, K. S., Haddad, I. E., and Baltensperger, U.:
874 Large contribution to secondary organic aerosol from isoprene cloud chemistry, *Science*
875 *Advances*, 7, eabe2952, 10.1126/sciadv.abe2952, 2021.
- 876 Levine, J. S.: The 1997 fires in Kalimantan and Sumatra, Indonesia: Gaseous and particulate
877 emissions, *Geophys. Res. Lett.*, 26, 815-818, 10.1029/1999GL900067, 1999.
- 878 Lim, Y., Tan, Y., and Turpin, B.: Chemical insights, explicit chemistry, and yields of secondary
879 organic aerosol from OH radical oxidation of methylglyoxal and glyoxal in the aqueous phase,
880 *Atmos. Chem. Phys.*, 13, 8651-8667, 10.5194/acp-13-8651-2013, 2013.



- 881 Liu, T., Chan, A. W., and Abbatt, J. P.: Multiphase oxidation of sulfur dioxide in aerosol
882 particles: Implications for sulfate formation in polluted environments, *Environ. Sci. Technol.*, 55,
883 4227-4242, 10.1021/acs.est.0c06496, 2021.
- 884 Löflund, M., Kasper-Giebl, A., Schuster, B., Giebl, H., Hitzenberger, R., and Puxbaum, H.:
885 Formic, acetic, oxalic, malonic and succinic acid concentrations and their contribution to organic
886 carbon in cloud water, *Atmos. Environ.*, 36, 1553-1558, 10.1016/S1352-2310(01)00573-8, 2002.
- 887 Lynch, P., Reid, J. S., Westphal, D. L., Zhang, J., Hogan, T. F., Hyer, E. J., Curtis, C. A., Hegg,
888 D. A., Shi, Y., Campbell, J. R., Rubin, J. I., Sessions, W. R., Turk, F. J., and Walker, A. L.: An
889 11-year global gridded aerosol optical thickness reanalysis (v1.0) for atmospheric and climate
890 sciences, *Geosci. Model Dev.*, 9, 1489-1522, 10.5194/gmd-9-1489-2016, 2016.
- 891 Ma, L., Dadashazar, H., Hilario, M. R. A., Cambaliza, M. O., Lorenzo, G. R., Simpas, J. B.,
892 Nguyen, P., and Sorooshian, A.: Contrasting wet deposition composition between three diverse
893 islands and coastal North American sites, *Atmos. Environ.*, 244, 117919,
894 10.1016/j.atmosenv.2020.117919, 2021.
- 895 MacDonald, A. B., Hossein Mardi, A., Dadashazar, H., Azadi Aghdam, M., Crosbie, E., Jonsson,
896 H. H., Flagan, R. C., Seinfeld, J. H., and Sorooshian, A.: On the relationship between cloud
897 water composition and cloud droplet number concentration, *Atmos. Chem. Phys.*, 20, 7645-7665,
898 10.5194/acp-20-7645-2020, 2020.
- 899 Mardi, A. H., Dadashazar, H., MacDonald, A. B., Crosbie, E., Coggon, M. M., Aghdam, M. A.,
900 Woods, R. K., Jonsson, H. H., Flagan, R. C., Seinfeld, J. H., and Sorooshian, A.: Effects of
901 biomass burning on stratocumulus droplet characteristics, drizzle rate, and composition, *J.*
902 *Geophys. Res. Atmos.*, 124, 12301-12318, 10.1029/2019JD031159, 2019.
- 903 Marinoni, A., Laj, P., Sellegri, K., and Mailhot, G.: Cloud chemistry at the Puy de Dôme:
904 variability and relationships with environmental factors, *Atmos. Chem. Phys.*, 4, 715-728,
905 10.5194/acp-4-715-2004, 2004.
- 906 McNaughton, C. S., Clarke, A. D., Howell, S. G., Pinkerton, M., Anderson, B., Thornhill, L.,
907 Hudgins, C., Winstead, E., Dibb, J. E., Scheuer, E., and Maring, H.: Results from the DC-8 Inlet
908 Characterization Experiment (DICE): Airborne versus surface sampling of mineral dust and sea
909 salt aerosols, *Aerosol Sci. Tech.*, 41, 136-159, 10.1080/02786820601118406, 2007.
- 910 Mochida, M., Umemoto, N., Kawamura, K., and Uematsu, M.: Bimodal size distribution of C2-
911 C4 dicarboxylic acids in the marine aerosols, *Geophys. Res. Lett.*, 30, 1672,
912 10.1029/2003gl017451, 2003.
- 913 Narukawa, M., Kawamura, K., Takeuchi, N., and Nakajima, T.: Distribution of dicarboxylic
914 acids and carbon isotopic compositions in aerosols from 1997 Indonesian forest fires, *Geophys.*
915 *Res. Lett.*, 26, 3101-3104, 10.1029/1999gl010810, 1999.
- 916 Page, S. E., Siegert, F., Rieley, J. O., Boehm, H.-D. V., Jaya, A., and Limin, S.: The amount of
917 carbon released from peat and forest fires in Indonesia during 1997, *Nature*, 420, 61-65,
918 10.1038/nature01131, 2002.



- 919 PSA: Highlights of the Philippine population 2015 census of population:
920 <https://psa.gov.ph/content/highlights-philippine-population-2015-census-population>, access:
921 January 7, 2016.
- 922 Raja, S., Raghunathan, R., Yu, X.-Y., Lee, T., Chen, J., Kommalapati, R. R., Murugesan, K.,
923 Shen, X., Qingzhong, Y., Valsaraj, K. T., and Collett Jr., J. L.: Fog chemistry in the Texas–
924 Louisiana gulf coast corridor, *Atmos. Environ.*, 42, 2048-2061, 10.1016/j.atmosenv.2007.12.004,
925 2008.
- 926 Raja, S., Raghunathan, R., Kommalapati, R. R., Shen, X., Collett Jr., J. L., and Valsaraj, K. T.:
927 Organic composition of fogwater in the Texas–Louisiana gulf coast corridor, *Atmos. Environ.*,
928 43, 4214-4222, 10.1016/j.atmosenv.2009.05.029, 2009.
- 929 Reid, J. S., Hobbs, P. V., Ferek, R. J., Blake, D. R., Martins, J. V., Dunlap, M. R., and Liousse,
930 C.: Physical, chemical, and optical properties of regional hazes dominated by smoke in Brazil, *J.*
931 *Geophys. Res. Atmos.*, 103, 32059-32080, 10.1029/98jd00458, 1998.
- 932 Reid, J. S., Hyer, E. J., Johnson, R. S., Holben, B. N., Yokelson, R. J., Zhang, J., Campbell, J. R.,
933 Christopher, S. A., Di Girolamo, L., Giglio, L., Holz, R. E., Kearney, C., Miettinen, J., Reid, E.
934 A., Turk, F. J., Wang, J., Xian, P., Zhao, G., Balasubramanian, R., Chew, B. N., Janjai, S.,
935 Lagrosas, N., Lestari, P., Lin, N.-H., Mahmud, M., Nguyen, A. X., Norris, B., Oanh, N. T. K.,
936 Oo, M., Salinas, S. V., Welton, E. J., and Liew, S. C.: Observing and understanding the
937 Southeast Asian aerosol system by remote sensing: An initial review and analysis for the Seven
938 Southeast Asian Studies (7SEAS) program, *Atmos. Res.*, 122, 403-468,
939 10.1016/j.atmosres.2012.06.005, 2013.
- 940 Reid, J. S., Lagrosas, N. D., Jonsson, H. H., Reid, E. A., Sessions, W. R., Simpas, J. B., Uy, S.
941 N., Boyd, T., Atwood, S. A., Blake, D. R., Campbell, J. R., Cliff, S. S., Holben, B. N., Holz, R.
942 E., Hyer, E. J., Lynch, P., Meinardi, S., Posselt, D. J., Richardson, K. A., Salinas, S. V., Smirnov,
943 A., Wang, Q., Yu, L., and Zhang, J.: Observations of the temporal variability in aerosol
944 properties and their relationships to meteorology in the summer monsoonal South China Sea/East
945 Sea: the scale-dependent role of monsoonal flows, the Madden–Julian Oscillation, tropical
946 cyclones, squall lines and cold pools, *Atmos. Chem. Phys.*, 15, 1745-1768, 10.5194/acp-15-
947 1745-2015, 2015.
- 948 Reid, J. S., Xian, P., Holben, B. N., Hyer, E. J., Reid, E. A., Salinas, S. V., Zhang, J., Campbell,
949 J. R., Chew, B. N., Holz, R. E., Kuciauskas, A. P., Lagrosas, N., Posselt, D. J., Sampson, C. R.,
950 Walker, A. L., Welton, E. J., and Zhang, C.: Aerosol meteorology of the Maritime Continent for
951 the 2012 7SEAS southwest monsoon intensive study – Part 1: regional-scale phenomena, *Atmos.*
952 *Chem. Phys.*, 16, 14041-14056, 10.5194/acp-16-14041-2016, 2016.
- 953 Reyes-Rodríguez, G. J., Gioda, A., Mayol-Bracero, O. L., and Collett Jr., J.: Organic carbon,
954 total nitrogen, and water-soluble ions in clouds from a tropical montane cloud forest in Puerto
955 Rico, *Atmos. Environ.*, 43, 4171-4177, 10.1016/j.atmosenv.2009.05.049, 2009.
- 956 Rinaldi, M., Decesari, S., Carbone, C., Finessi, E., Fuzzi, S., Ceburnis, D., O'Dowd, C. D.,
957 Sciare, J., Burrows, J. P., Vrekoussis, M., Ervens, B., Tsigaridis, K., and Facchini, M. C.:



- 958 Evidence of a natural marine source of oxalic acid and a possible link to glyoxal, *J. Geophys.*
959 *Res. Atmos.*, 116, D16204, 10.1029/2011JD015659, 2011.
- 960 Rogge, W. F., Mazurek, M. A., Hildemann, L. M., Cass, G. R., and Simoneit, B. R. T.:
961 Quantification of urban organic aerosols at a molecular level: Identification, abundance and
962 seasonal variation, *Atmos. Environ. A-Gen.*, 27, 1309-1330, 10.1016/0960-1686(93)90257-y,
963 1993.
- 964 Rolph, G., Stein, A., and Stunder, B.: Real-time Environmental Applications and Display
965 sYstem: READY, *Environ. Modell. Softw.*, 95, 210-228, 10.1016/j.envsoft.2017.06.025, 2017.
- 966 Saltzman, E. S., Savoie, D. L., Zika, R. G., and Prospero, J. M.: Methane sulfonic acid in the
967 marine atmosphere, *J. Geophys. Res. Oceans*, 88, 10897-10902, 10.1029/JC088iC15p10897,
968 1983.
- 969 Seinfeld, J. H., and Pandis, S. N.: *Atmospheric Chemistry and Physics*, 3rd ed., Wiley-
970 Interscience, New York, NY, 2016.
- 971 Shen, X.: Aqueous Phase Sulfate Production in Clouds at Mt. Tai in Eastern China, Ph.D.,
972 Atmospheric Science, Colorado State University, Fort Collins, 193 pp., 2011.
- 973 Shingler, T., Dey, S., Sorooshian, A., Brechtel, F., Wang, Z., Metcalf, A., Coggon, M.,
974 Muehnenstaedt, J., Russell, L., Jonsson, H., and Seinfeld, J. H.: Characterisation and airborne
975 deployment of a new counterflow virtual impactor inlet, *Atmos. Meas. Tech.*, 5, 1259-1269,
976 10.5194/amt-5-1259-2012, 2012.
- 977 Sorooshian, A., Varutbangkul, V., Brechtel, F. J., Ervens, B., Feingold, G., Bahreini, R.,
978 Murphy, S. M., Holloway, J. S., Atlas, E. L., Buzorius, G., Jonsson, H., Flagan, R. C., and
979 Seinfeld, J. H.: Oxalic acid in clear and cloudy atmospheres: Analysis of data from International
980 Consortium for Atmospheric Research on Transport and Transformation 2004, *J. Geophys. Res.*
981 *Atmos.*, 111, D23S45, 10.1029/2005jd006880, 2006.
- 982 Sorooshian, A., Crosbie, E., Maudlin, L. C., Youn, J. S., Wang, Z., Shingler, T., Ortega, A. M.,
983 Hersey, S., and Woods, R. K.: Surface and airborne measurements of organosulfur and
984 methanesulfonate over the Western United States and coastal areas, *J. Geophys. Res. Atmos.*,
985 120, 8535-8548, 10.1002/2015JD023822, 2015.
- 986 Stahl, C., Cruz, M. T., Bañaga, P. A., Betito, G., Braun, R. A., Aghdam, M. A., Cambaliza, M.
987 O., Lorenzo, G. R., MacDonald, A. B., Hilario, M. R. A., Pabroa, P. C., Yee, J. R., Simpas, J. B.,
988 and Sorooshian, A.: Sources and characteristics of size-resolved particulate organic acids and
989 methanesulfonate in a coastal megacity: Manila, Philippines, *Atmos. Chem. Phys.*, 20, 15907-
990 15935, 10.5194/acp-20-15907-2020, 2020.
- 991 Stefan, M. I., Hoy, A. R., and Bolton, J. R.: Kinetics and mechanism of the degradation and
992 mineralization of acetone in dilute aqueous solution sensitized by the UV photolysis of hydrogen
993 peroxide, *Environ. Sci. Technol.*, 30, 2382-2390, 10.1021/es950866i, 1996.



- 994 Stein, A. F., Draxler, R. R., Rolph, G. D., Stunder, B. J. B., Cohen, M. D., and Ngan, F.:
995 NOAA's HYSPLIT Atmospheric Transport and Dispersion Modeling System, *B. Am. Meteorol.*
996 *Soc.*, 96, 2059-2077, 10.1175/bams-d-14-00110.1, 2015.
- 997 Stockwell, C. E., Jayarathne, T., Cochrane, M. A., Ryan, K. C., Putra, E. I., Saharjo, B. H.,
998 Nurhayati, A. D., Albar, I., Blake, D. R., Simpson, I. J., Stone, E. A., and Yokelson, R. J.: Field
999 measurements of trace gases and aerosols emitted by peat fires in Central Kalimantan, Indonesia,
1000 during the 2015 El Niño, *Atmos. Chem. Phys.*, 16, 11711-11732, 10.5194/acp-16-11711-2016,
1001 2016.
- 1002 Straub, D. J., Lee, T., and Collett Jr., J. L.: Chemical composition of marine stratocumulus
1003 clouds over the eastern Pacific Ocean, *J. Geophys. Res. Atmos.*, 112, D04307,
1004 10.1029/2006JD007439, 2007.
- 1005 Straub, D. J., Hutchings, J. W., and Herckes, P.: Measurements of fog composition at a rural site,
1006 *Atmos. Environ.*, 47, 195-205, 10.1016/j.atmosenv.2011.11.014, 2012.
- 1007 Straub, D. J.: Radiation fog chemical composition and its temporal trend over an eight year
1008 period, *Atmos. Environ.*, 148, 49-61, 10.1016/j.atmosenv.2016.10.031, 2017.
- 1009 Sullivan, R. C., and Prather, K. A.: Investigations of the diurnal cycle and mixing state of oxalic
1010 acid in individual particles in Asian aerosol outflow, *Environ. Sci. Technol.*, 41, 8062-8069,
1011 10.1021/es071134g, 2007.
- 1012 Talbot, R., Beecher, K., Harriss, R., and Cofer III, W.: Atmospheric geochemistry of formic and
1013 acetic acids at a mid-latitude temperate site, *J. Geophys. Res. Atmos.*, 93, 1638-1652,
1014 10.1029/JD093iD02p01638, 1988.
- 1015 Tan, Y., Carlton, A. G., Seitzinger, S. P., and Turpin, B. J.: SOA from methylglyoxal in clouds
1016 and wet aerosols: Measurement and prediction of key products, *Atmos. Environ.*, 44, 5218-5226,
1017 10.1016/j.atmosenv.2010.08.045, 2010.
- 1018 Thomas, D. A., Coggon, M. M., Lignell, H., Schilling, K. A., Zhang, X., Schwantes, R. H.,
1019 Flagan, R. C., Seinfeld, J. H., and Beauchamp, J. L.: Real-time studies of iron oxalate-mediated
1020 oxidation of glycolaldehyde as a model for photochemical aging of aqueous tropospheric
1021 aerosols, *Environ. Sci. Technol.*, 50, 12241-12249, 10.1021/acs.est.6b03588, 2016.
- 1022 Tsai, Y. I., Sopajaree, K., Chotruksa, A., Wu, H.-C., and Kuo, S.-C.: Source indicators of
1023 biomass burning associated with inorganic salts and carboxylates in dry season ambient aerosol
1024 in Chiang Mai Basin, Thailand, *Atmos. Environ.*, 78, 93-104, 10.1016/j.atmosenv.2012.09.040,
1025 2013.
- 1026 Turekian, V. C., Macko, S. A., and Keene, W. C.: Concentrations, isotopic compositions, and
1027 sources of size-resolved, particulate organic carbon and oxalate in near-surface marine air at
1028 Bermuda during spring, *J. Geophys. Res. Atmos.*, 108, 4157, 10.1029/2002JD002053, 2003.



- 1029 Turpin, B. J., and Lim, H.-J.: Species contributions to PM_{2.5} mass concentrations: Revisiting
1030 common assumptions for estimating organic mass, *Aerosol Sci. Tech.*, 35, 602-610,
1031 10.1080/02786820119445, 2001.
- 1032 Wang, J., Ge, C., Yang, Z., Hyer, E. J., Reid, J. S., Chew, B.-N., Mahmud, M., Zhang, Y., and
1033 Zhang, M.: Mesoscale modeling of smoke transport over the Southeast Asian Maritime
1034 Continent: Interplay of sea breeze, trade wind, typhoon, and topography, *Atmos. Res.*, 122, 486-
1035 503, 10.1016/j.atmosres.2012.05.009, 2013.
- 1036 Wang, Y., Zhuang, G., Chen, S., An, Z., and Zheng, A.: Characteristics and sources of formic,
1037 acetic and oxalic acids in PM_{2.5} and PM₁₀ aerosols in Beijing, China, *Atmos. Res.*, 84, 169-
1038 181, 10.1016/j.atmosres.2006.07.001, 2007.
- 1039 Wang, Y., Guo, J., Wang, T., Ding, A., Gao, J., Zhou, Y., Collett Jr., J. L., and Wang, W.:
1040 Influence of regional pollution and sandstorms on the chemical composition of cloud/fog at the
1041 summit of Mt. Taishan in northern China, *Atmos. Res.*, 99, 434-442,
1042 10.1016/j.atmosres.2010.11.010, 2011.
- 1043 Xian, P., Reid, J. S., Atwood, S. A., Johnson, R. S., Hyer, E. J., Westphal, D. L., and Sessions,
1044 W.: Smoke aerosol transport patterns over the Maritime Continent, *Atmos. Res.*, 122, 469-485,
1045 10.1016/j.atmosres.2012.05.006, 2013.
- 1046 Yang, F., Gu, Z., Feng, J., Liu, X., and Yao, X.: Biogenic and anthropogenic sources of oxalate
1047 in PM_{2.5} in a mega city, Shanghai, *Atmos. Res.*, 138, 356-363, 10.1016/j.atmosres.2013.12.006,
1048 2014.
- 1049 Yao, L., Yang, L., Chen, J., Wang, X., Xue, L., Li, W., Sui, X., Wen, L., Chi, J., and Zhu, Y.:
1050 Characteristics of carbonaceous aerosols: Impact of biomass burning and secondary formation in
1051 summertime in a rural area of the North China Plain, *Sci. Total Environ.*, 557-558, 520-530,
1052 10.1016/j.scitotenv.2016.03.111, 2016.
- 1053 Youn, J.-S., Crosbie, E., Maudlin, L., Wang, Z., and Sorooshian, A.: Dimethylamine as a major
1054 alkyl amine species in particles and cloud water: Observations in semi-arid and coastal regions,
1055 *Atmos. Environ.*, 122, 250-258, 10.1016/j.atmosenv.2015.09.061, 2015.
- 1056 Yuan, H., Wang, Y., and Zhuang, G.: MSA in Beijing aerosol, *Chinese Sci. Bull.*, 49, 1020-
1057 1025, 10.1007/bf03184031, 2004.
- 1058 Zhang, Q., and Anastasio, C.: Chemistry of fog waters in California's Central Valley—Part 3:
1059 concentrations and speciation of organic and inorganic nitrogen, *Atmos. Environ.*, 35, 5629-
1060 5643, 10.1016/S1352-2310(01)00337-5, 2001.
- 1061 Zhang, Q., Worsnop, D., Canagaratna, M., and Jimenez, J.: Hydrocarbon-like and oxygenated
1062 organic aerosols in Pittsburgh: insights into sources and processes of organic aerosols, *Atmos.*
1063 *Chem. Phys.*, 5, 3289-3311, 10.5194/acp-5-3289-2005, 2005.



1064 Ziemba, L. D., Griffin, R. J., Whitlow, S., and Talbot, R. W.: Characterization of water-soluble
1065 organic aerosol in coastal New England: Implications of variations in size distribution, *Atmos.*
1066 *Environ.*, 45, 7319-7329, 10.1016/j.atmosenv.2011.08.022, 2011.

1067

1068



1069 **Table 1:** Mass concentration limits of detection (LOD), minimum, maximum, mean, one
 1070 standard deviation, and median values (ppb; left), in addition to mass fraction (%; right) for the
 1071 159 CAMP²Ex cloud water samples with TOC data; note that mass fraction values depend on the
 1072 C mass of each organic species shown. Total measured mass is defined as the sum of TOM, Na⁺,
 1073 NH₄⁺, K⁺, Mg²⁺, Ca²⁺, Cl⁻, NO₂⁻, Br⁻, NO₃⁻, and SO₄²⁻. MCA – monocarboxylic acids, DCA –
 1074 dicarboxylic acids, MSA – methanesulfonate, DMA – dimethylamine, MO – measured organics,
 1075 TOM – total organic matter, DL – detection limit.

	LOD	Concentration (ppb)					Mass Fraction (%)				
		Min	Max	Median	Mean	Stdev	Min	Max	Median	Mean	Stdev
Glycolate	98.76	<DL	224.8	10.7	13.5	20.3	0.0	35.0	0.6	1.3	3.7
Acetate	6.38	<DL	3926.0	159.4	251.4	409.9	0.0	100.0	10.5	14.7	20.5
Formate	19.77	2.1	3819.0	66.6	188.5	432.5	0.2	100.0	3.8	5.4	9.3
Pyruvate	5.45	<DL	296.9	5.4	24.4	41.3	0.0	56.1	0.5	1.3	4.5
MCA	-	13.4	8041.9	253.4	477.8	857.8	0.6	100.0	16.9	22.6	33.9
Glutarate	43.70	<DL	258.7	<DL	6.8	27.3	0.0	1.0	0.0	0.1	0.2
Adipate	39.21	<DL	71.5	3.0	5.3	8.3	0.0	43.7	0.4	1.0	3.6
Succinate	38.64	<DL	1372.0	<DL	55.2	137.7	0.0	9.3	0.0	1.6	2.4
Maleate	14.81	<DL	14.7	<DL	0.7	2.3	0.0	0.8	0.0	0.0	0.1
Oxalate	55.23	<DL	1135.0	38.6	95.6	148.2	0.0	43.9	1.7	2.8	4.3
DCA	-	1.5	2765.7	61.4	163.7	295.3	0.1	69.8	3.3	5.5	7.5
MSA	88.01	<DL	24.8	3.9	5.1	5.3	0.0	0.9	0.1	0.1	0.1
DMA	56.97	<DL	183.8	<DL	11.2	32.4	0.0	45.3	0.0	1.7	6.3
MO	-	29.5	10815.3	334.3	657.7	1124.7	1.5	100.0	23.8	30.0	41.2
TOC	0.05	18	13660	546	902	1435	↑ Relative to TOC (%) ↑				
Inorg/TOM	-	0.1	90.3	3.3	5.8	8.6	↓ Relative to total measured concentrations (%) ↓				
MO	-	-	-	-	-	-	0.8	57.6	7.2	10.3	9.2
TOM	-	32	24588	983	1624	2584	1.1	95.1	23.2	30.7	24.5
Inorganic	-	26	117933	3894	8651	13645	4.9	98.9	76.8	69.3	24.5
Na	16.62	<DL	29280	609	1650	3192	0.0	26.6	9.5	10.0	7.8
NH ₄	176.80	<DL	8099	427	804	1010	0.0	68.1	7.2	11.2	13.2
K	142.35	<DL	1211	21	75	144	0.0	21.8	0.5	0.8	2.0
Mg	46.20	<DL	3701	58	182	379	0.0	4.0	1.0	1.1	0.9
Ca	74.81	<DL	1951	118	201	277	0.0	25.2	1.6	3.5	4.6
Cl	76.59	<DL	38200	908	2451	4438	0.0	42.7	15.3	16.0	11.7
NO ₂	46.24	<DL	16	<DL	2	3	0.0	0.4	0.0	0.0	0.1
Br	7.82	<DL	44	1	4	7	0.0	0.2	0.0	0.0	0.0
NO ₃	17.33	<DL	26560	572	1488	2925	0.0	43.4	10.4	12.6	8.2
SO ₄	414.73	2	15680	868	1795	2495	0.4	34.9	14.1	14.0	8.5

1076

1077



Table 2: Speciated concentrations of organics (ppb) for each case study, where the first group of rows are monocarboxylic acids (MCA), the second group of rows are dicarboxylic acids (DCA), the third group of rows are other organics plus total measured organics (MO) and total organic carbon (TOC), inorganic ions, and the fifth group are select ratios. n = number of samples.

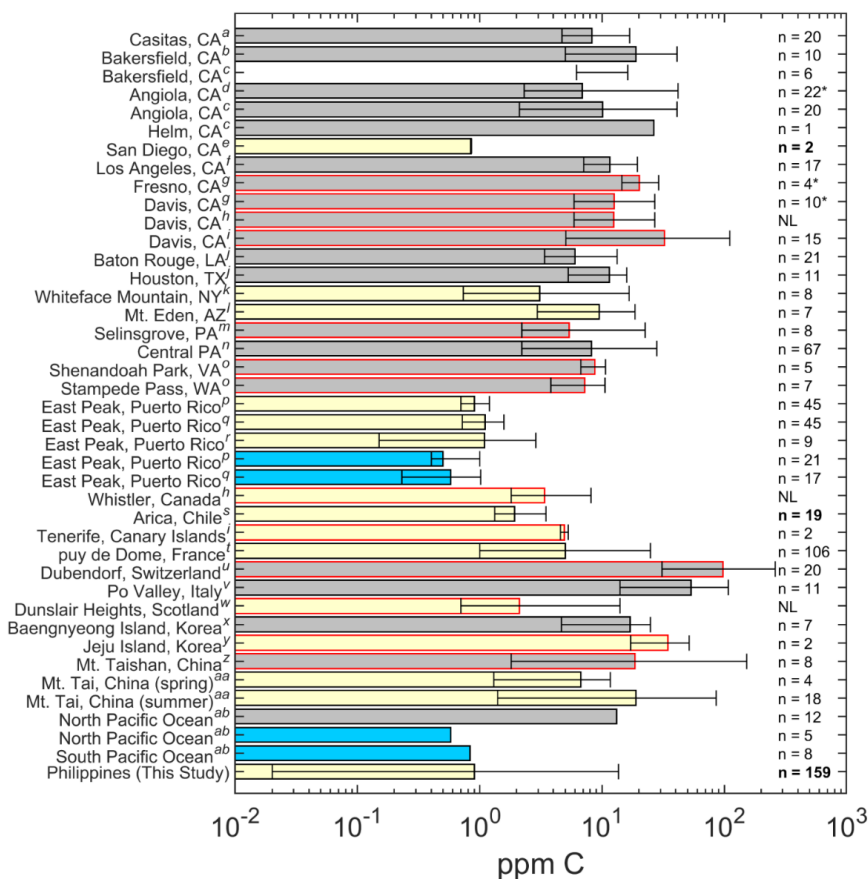
	North (n = 20)					East (n = 11)					Biomass Burning (n = 4)					Clark (n = 25)				
	Min	Max	Median	Mean	Stdev	Min	Max	Median	Mean	Stdev	Min	Max	Median	Mean	Stdev	Min	Max	Median	Mean	Stdev
Glycolate	5.96	37.18	15.80	17.59	9.15	5.34	30.00	12.21	13.68	7.25	<DL	46.86	7.20	15.31	22.10	<DL	53.42	6.90	11.68	14.61
Acetate	1.94	288.80	184.85	177.82	72.96	301.70	423.50	358.60	359.04	40.71	47.85	3926.00	1703.50	1845.21	1667.91	<DL	1105.00	185.20	296.65	325.80
Formate	10.28	232.20	62.66	83.16	79.65	61.02	492.80	248.30	258.18	122.19	151.00	3819.00	2370.00	2177.50	1588.91	2.42	1041.00	152.00	266.05	316.80
Pyruvate	2.14	126.50	35.91	42.98	38.98	7.50	78.24	24.65	32.25	21.01	<DL	296.90	103.41	125.93	126.12	1.07	161.80	16.08	30.31	35.84
MCA	25.32	632.19	299.90	321.55	183.61	431.25	923.72	673.22	663.15	142.72	245.71	8041.90	4184.11	4163.96	3335.76	31.93	2066.20	369.18	604.69	641.90
Glutarate	<DL	10.18	<DL	1.53	2.76	<DL	10.86	4.07	5.12	3.67	62.46	258.70	140.20	150.39	82.20	<DL	62.46	1.36	9.42	16.85
Adipate	<DL	17.44	<DL	5.15	6.27	<DL	<DL	<DL	<DL	<DL	<DL	<DL	<DL	<DL	<DL	<DL	37.43	<DL	3.78	7.89
Succinate	<DL	136.20	28.09	42.30	47.84	15.45	176.90	63.90	74.11	57.27	24.58	1372.00	415.70	557.00	575.65	<DL	498.50	18.96	67.74	123.72
Malate	<DL	<DL	<DL	<DL	<DL	<DL	<DL	<DL	<DL	<DL	<DL	11.61	5.36	5.58	6.46	<DL	14.73	<DL	2.71	4.17
Oxalate	37.53	330.40	124.75	148.67	81.47	52.51	311.20	123.30	153.63	81.06	303.80	1135.00	520.05	619.73	360.12	5.55	448.90	43.63	88.33	103.88
DCA	67.84	467.09	149.27	197.64	125.25	80.60	493.36	194.12	232.86	136.37	735.78	2765.70	914.65	1332.69	968.88	7.67	1009.86	72.10	171.99	238.04
MSA	1.55	14.72	7.75	8.29	3.16	3.10	17.82	10.07	10.57	4.40	<DL	24.79	3.87	8.13	11.69	<DL	10.85	3.87	4.18	3.62
DMA	<DL	<DL	<DL	<DL	<DL	<DL	<DL	<DL	<DL	<DL	<DL	<DL	<DL	<DL	<DL	<DL	61.25	<DL	6.45	15.89
MO	99.36	1088.83	483.78	527.48	301.59	567.01	1364.27	855.59	906.58	269.42	1016.58	10815.35	5093.60	5504.78	4186.65	54.05	3053.76	433.14	787.32	837.34
TOC	364	1085	555	636	230	663	1570	985	1051	331	4974	13660	7366	8342	3730	220	3362	849	1181	920
Na	693	11870	2273	3238	2861	618	6546	1970	2569	1738	833	4425	2160	2394	1624	12	5870	625	1105	1403
NH ₄	181	1955	644	847	515	513	2379	1307	1432	587	2517	8099	3685	4496	2483	45	2880	947	1009	815
K	14	405	50	89	100	18	493	66	123	136	132	724	272	350	258	2	264	32	63	76
Mg	41	1338	236	347	328	62	668	209	273	183	84	501	242	267	191	<DL	631	65	117	153
Ca	<DL	765	97	174	219	49	778	167	269	219	106	534	236	278	210	39	904	177	230	184
Cl	1445	18520	3772	5277	4333	900	8357	2760	3510	2196	1126	5989	2553	3055	2124	45	9083	991	1716	2107
NO ₂	<DL	<DL	<DL	<DL	<DL	<DL	<DL	<DL	<DL	<DL	<DL	6	1	2	3	<DL	16	<DL	3	5
Br	3	36	13	16	8	2	7	4	4	1	1	6	2	3	2	<DL	13	1	3	3
NO ₃	477	5265	1197	1810	1506	1084	8724	2902	3772	2296	1880	7045	3344	3903	2277	65	2759	691	931	736
SO ₄	1305	12120	3281	4503	2865	1212	5296	2819	3223	1385	2313	9993	4177	5165	3343	23	4406	1157	1416	1157
Acc/For	0.19	9.66	2.65	4.21	3.26	0.75	5.67	1.52	1.93	1.51	0.32	1.03	0.70	0.69	0.30	0	3.86	0.98	1.12	0.84
Cl/Na	1.52	2.08	1.69	1.70	0.13	1.28	1.51	1.40	1.40	0.06	1.07	1.43	1.35	1.30	0.16	1.38	3.70	1.69	1.84	0.56
Ca/Na	0	0.08	0.04	0.04	0.02	0.05	0.14	0.10	0.10	0.03	0.08	0.13	0.12	0.11	0.02	0.05	6.17	0.32	0.99	1.46
K/Na	0.02	0.03	0.02	0.02	0.01	0.03	0.08	0.04	0.04	0.01	0.10	0.18	0.16	0.15	0.04	0.01	3.93	0.05	0.25	0.78
MO/TOC	0.07	0.37	0.29	0.27	0.08	0.18	0.42	0.29	0.31	0.07	0.04	0.28	0.26	0.21	0.11	0.03	0.57	0.19	0.20	0.13



1079 **Table 3:** Average organic composition for each case study where the first, second, and third
 1080 group of rows show percentage contribution (%) of individual components to monocarboxylic
 1081 acids (MCA), dicarboxylic acids (DCA), and total organic carbon (TOC), respectively.

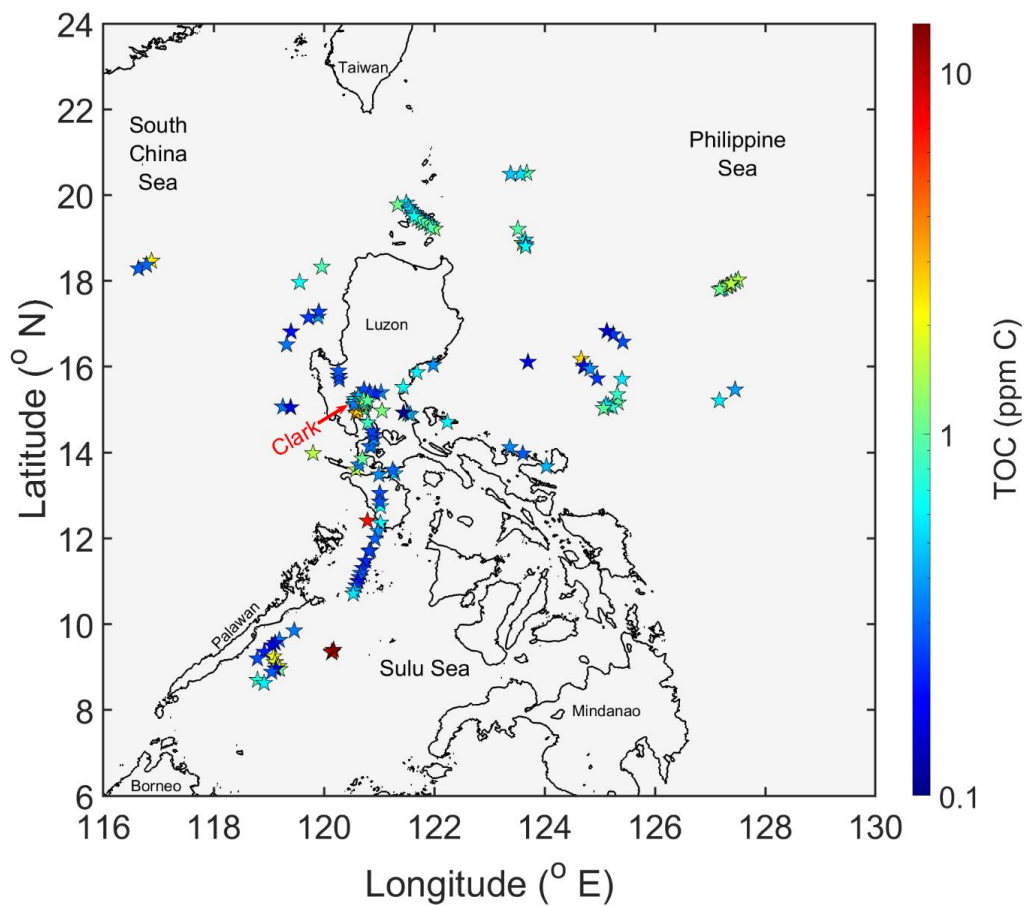
Group	Species (%)	North (n = 20)		East (n = 11)		BB (n = 4)		Clark (n = 25)	
		Mean	Stdev	Mean	Stdev	Mean	Stdev	Mean	Stdev
MCA	Glycolate	7.20	9.20	1.84	0.81	5.09	9.87	17.65	29.05
	Acetate	64.03	17.74	64.20	10.85	45.86	14.07	46.35	23.98
	Formate	16.54	9.83	28.62	10.35	46.40	7.24	29.09	11.72
	Pyruvate	12.23	6.90	5.33	2.87	2.65	1.87	6.91	4.90
DCA	Glutarate	0.65	1.00	2.91	1.41	17.15	9.28	4.02	5.02
	Adipate	8.04	9.47	0	0	0	0	16.05	21.48
	Succinate	20.82	20.08	38.52	12.15	41.95	25.27	26.53	25.39
	Maleate	0	0	0	0	0.75	0.88	3.20	5.93
	Oxalate	70.49	12.29	58.57	11.52	40.16	16.50	50.20	17.42
TOC	MSA	0.17	0.05	0.13	0.04	0.01	0.02	0.06	0.07
	DMA	0	0	0	0	0	0	0.43	1.17
	MCA	17.79	6.17	23.66	5.99	16.03	10.13	16.28	11.91
	DCA	8.75	2.65	6.82	2.94	5.21	1.60	3.70	2.67
	MO	26.72	7.86	30.61	7.35	21.25	11.32	20.46	13.34
	Undetected	73.28	7.86	69.39	7.35	78.75	11.32	79.54	13.34

1082



1083

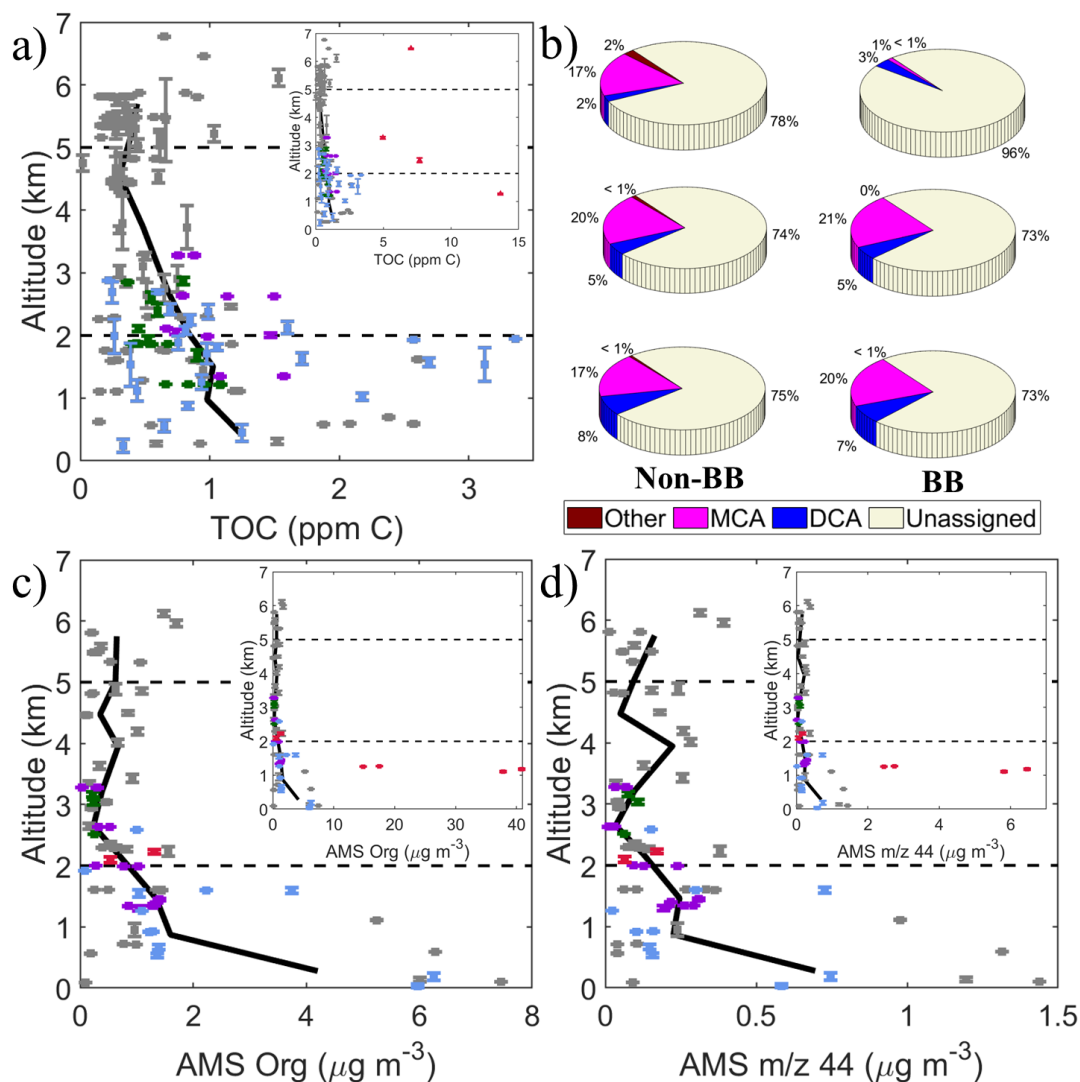
1084 **Figure 1:** TOC (or DOC if TOC values were unavailable) concentrations reported for past
 1085 studies in relation to this work organized by continent. Bars represent the average values and the
 1086 error bars represent the minimum and maximum values. The absence of a solid bar means no
 1087 average was available. No error bars means there was no range given, and * indicates the median
 1088 value was reported rather than an average. Gray, yellow, and blue bars represent studies looking
 1089 at fog, clouds, and rain, respectively. Bars that are outlined in black are studies that used TOC
 1090 and bars outlined in red are studies that used DOC. The n values represent the number of samples
 1091 used in the study and NL means the number of samples were not listed. Bolded n values denote
 1092 airborne samples. (a - Boris et al. (2018), b - Collett Jr. et al. (1998), c - Herckes et al. (2002), d -
 1093 Herckes et al. (2007), e - Straub et al. (2007), f - Erel et al. (1993), g - Ehrenhauser et al. (2012),
 1094 h - Ervens et al. (2013), i - Zhang and Anastasio (2001), j - Raja et al. (2008), k - Cook et al.
 1095 (2017), l - Hutchings et al. (2008), m - Straub et al. (2012), n - Straub (2017), o - Anastasio et al.
 1096 (1994), p - Gioda et al. (2011), q - Gioda et al. (2008), r - Reyes-Rodríguez et al. (2009), s -
 1097 Benedict et al. (2012), t - Deguillaume et al. (2014), u - Capel et al. (1990), v - Gelencser et al.
 1098 (2000), w - Hadi et al. (1995), x - Boris et al. (2016), y - Decesari et al. (2005), z - Wang et al.
 1099 (2011), aa - Shen (2011), ab - Kim et al. (2020))



1100

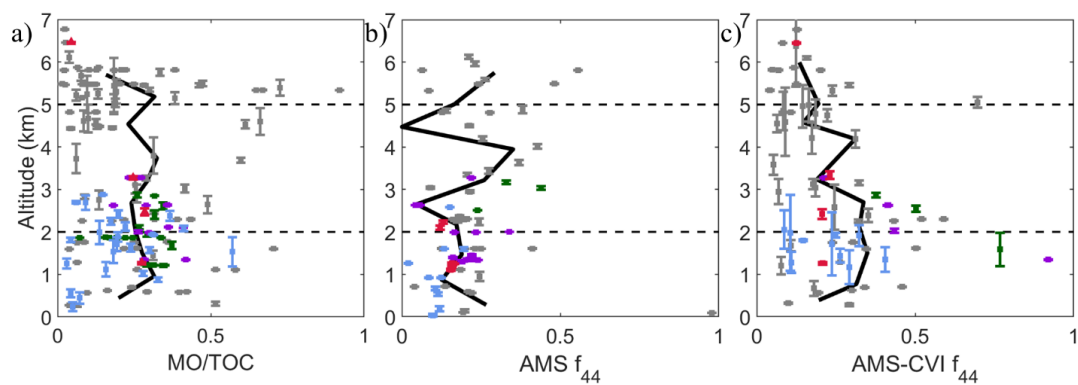
1101 **Figure 2:** Map of sample region where the stars represent the midpoint of the cloud water
1102 samples where total organic carbon (TOC) was measured. Stars are colored by TOC on a
1103 logarithmic scale.

1104



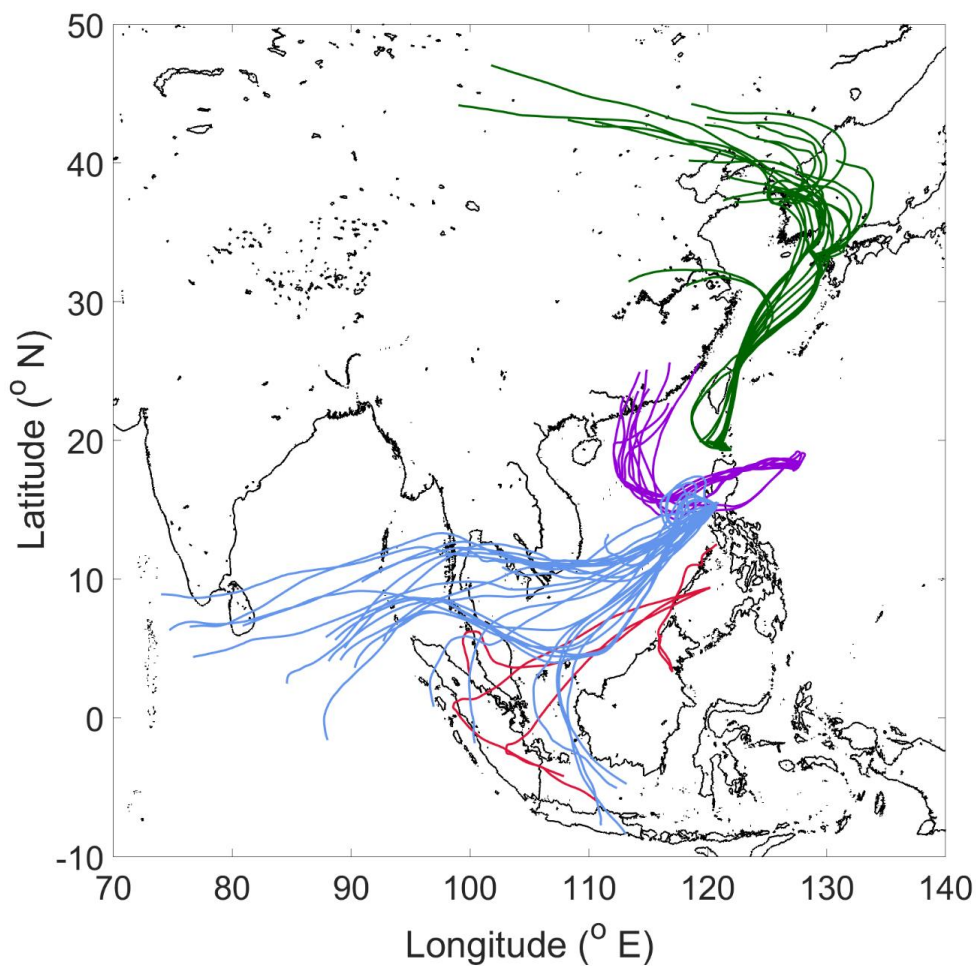
1105

1106 **Figure 3.** (a) Vertical profile of TOC concentrations ($n = 159$ samples) with the smaller inset
 1107 including four samples with enhanced TOC owing to biomass burning (BB) influence. (b) Mass
 1108 fractions of different subsets of species contributing to TOC at high (> 5 km), mid (2 – 5 km),
 1109 and low (< 2 km) altitude with the beige area representing undetected species. Vertical profile of
 1110 AMS (c) organic and (d) m/z 44 corresponding to spatially and temporally adjacent cloud-free
 1111 periods of the collected cloud water samples. Colors in panels a/b/d represent the case study
 1112 points in Sect. 4: North (green), East (purple), Biomass Burning (red), Clark (blue), non-case
 1113 points (gray). The solid black lines in panels a/b/d represent locally-weighted average values.
 1114 The error bars represent one standard deviation of the altitude variance.



1115

1116 **Figure 4.** Vertical profile of (a) ratio of C mass from measured organics (MO) to TOC for cloud
1117 water samples, (b) AMS f_{44} in cloud-free air, and (c) AMS-CVI f_{44} in cloudy air. AMS data in (b)
1118 corresponds to cloud-free periods that were spatially and temporally adjacent to the collected
1119 cloud water samples, while those in (c) are within the period of cloud water collection times in
1120 cloud. Colors in panels a/b/d represent the same case study points as Figure 3: North (green),
1121 East (purple), Biomass Burning (red), Clark (blue), non-case points (gray). The black lines in
1122 panels a/b/d represent locally-weighted average values.



1123

1124 **Figure 5:** Spatial summary of 120-hour back trajectories for each sample included in respective
1125 case study sample sets: North (green; n = 20), East (purple; n = 11), Biomass Burning (red; n =
1126 4), and Clark (blue; n = 25).

1127